High Performance WLAN Using Smart Antenna

by

Hesham Hassan Banaser

A thesis
presented to the University of Waterloo
in fulfillment of the
thesis requirement for the degree of
Master of Applied Science
in
Electrical and Computer Engineering

Waterloo, Ontario, Canada, 2007

I hereby declare that I am the sole author of this thesis. This is a true copy of the thesis, including any required final revisions, as accepted by my examiners.

I understand that my thesis may be made electronically available to the public.

Abstract

The need for higher data rates in WLANs boosts drastically because tremendous consumer interest in emerging multimedia applications, such as HDTV, has been increased. Currently, the IEEE 802.11a/b/g WLANs provide a limited data rate for the current user application requirements. In order to overcome substantial limitations of the existing WLANs, the next generation of WLANs, IEEE 802.11n, is in the course of development and expected to support higher throughput, larger coverage area and better QoS. The high performance IEEE 802.11n WLAN can improve data rate significantly by using smart antenna systems in the physical layer to take advantage of multi-path fading of wireless channels.

In this thesis, an analytical model is developed to study the MAC performance and the underlying smart antenna technologies used in multi-path fading channels. Multiple antennas employed in the AP arise two popular approaches to provide a significant performance improvement, diversity and multiplexing. Considering the diversity gain of multiple antennas at the AP in which the AP with multiple antennas serves one user at a time, the capacity and throughput can be obtained. In addition, the AP is possible to serve multiple users in the downlink, by exploiting the multiplexing gain of the wireless channel. We investigate the maximum network throughput when the traffic intensity of the AP approaches to one. Unlike most of previous research which focus on either the physical or the MAC layer performance, our analytical model jointly considers the MAC protocol and the smart antenna technology.

Acknowledgements

I would like to express my deepest and sincere gratitude to my supervisor, Professor Xuemin (Sherman) Shen. His valuable support, guidance and encouragement were vital to achieving this degree. I am looking forward to continue with him my PhD studies.

I would also like to extend my appreciation to my thesis readers, Professor Liang-Liang Xie and Professor Sagar Naik, for reviewing my thesis and providing valuable suggestions and comments. Special thank goes to Lin Cai for her productive discussions and continuous feedback throughout this research. I am deeply indebted to all my colleagues in BBCR group. I am also grateful to the ECE department staff for their kind assistance and cooperation.

Special acknowledgment is due to the ministry of higher education in Saudi Arabia for granting me this scholarship, also for the generous support from the Saudi Arabian Cultural Bureau in Canada.

Finally, I want to thank my wonderful parents, siblings and friends for being patient with me in all their hardships that they incurred in my long absence, and for offering words of wit and encouragements. Many thanks go to everyone who contributed to make my Master's experience exceptional and very enjoyable journey.

To my parents...

Contents

List of Tables

List of Figures

List of Acronyms

WLANs	Wireless Local Area Networks
AP	Access Point
MN	Mobile Node
SISO	Single-Input Single-Output
SIMO	Single-Input Multiple-Output
MISO	Multiple-Input Single-Output
MIMO	Multiple-Input Multiple-Output
HDTV	High-Definition Television
QoS	Quality of Service
MAC	Medium Access Control
SAP	Service Access Point
DCF	Distributed Coordination Function
OFDM	Orthogonal Frequency Division Multiplexing
HiperLAN	High Performance Radio Local Area Network
CAC	Connection Admission Control
PCF	Point Coordination Function

BSS	Basic Service Set
IBSS	Independent Basic Service Set
DS	Distributed System
ESS	Extended Service Set
PLCP	Physical Layer Convergence Procedure
PMD	Physical Medium Dependent
FH or FHSS	Frequency Hopping Spread Spectrum
DS or DSSS	Direct Sequence Spread Spectrum
ERP	Extended Rate Physical
CCK	Complementary Code Keying
BPSK	Binary Phase Shift Keying
QPSK	Quadrature Phase Shift Keying
QAM	Quadrature Amplitude Modulation
SNR	Signal to Noise Ratio
BER	Bit Error Rate
CSMA/CA	Carrier Sense Multiple Access with Collision Avoidance
RTS/CTS	Request To Send/Clear To Send
NAV	Network Allocation Vector
DIFS	Distributed InterFrame Space
CW	Contention Window
ACK	Acknowledgement
SIFS	Short InterFrame Space
AWGN	Additive White Gaussian Noise

CDI	Channel Distribution Information
CSI	Channel State Information
MRC	Maximum Ratio Combining
SC	Selection Combining
STC	Space Time Coding
BLAST	Bell Laboratories Layered Space-Time
DPC	Dirty Paper Coding
CSIT	Channel State Information at Transmitter
CBR	Constant Bit Rate
EDCF	Enhanced Distributed InterFrame Space
HCF	Hybrid Coordination Function
TXOP	Transmission Opportunity

Chapter 1

Introduction

Wireless local area networks (WLANs) have been widely deployed for providing ubiquitous Internet access. IEEE 802.11 WLAN standards (e.g. 802.11b and 802.11a/g) can provide up to 11 Mbps and 54 Mbps data rates. However, the achievable throughput of a WLAN is below the half of these data rates because of wireless channel impairments and the protocol overheads. Moreover, the majority of existing WLANs are based on infrastructure mode in which an access point (AP) carries all traffics in the WLAN; hence, the AP becomes the system bottleneck due to the huge traffic load.

While emerging WLAN applications such as video conferencing and high-definition television (HDTV) require higher performance WLANs, the next generation IEEE 802.11n WLAN is in the course of development and expected to support higher throughput, larger coverage area and better quality of service (QoS). Beside considering backward compatibility with the current WLANs, the IEEE 802.11n aims to provide over 100 Mbps at the medium access control (MAC) data service access point (SAP) via physical (PHY) and

MAC enhancements. The IEEE 802.11n employs smart antenna systems (i.e. multiple-input multiple-output (MIMO) technology) to support physical layer raw data rate up to 600 Mbps.

Smart antenna systems are adopted by several wireless data communication standards. Employing multiple antennas at both transmitter and receiver improves system performance in terms of transmission rate and link reliability via multiplexing and diversity gains, respectively. The high performance IEEE 802.11n WLAN can improve data rate significantly by using smart antenna systems in the physical layer to take advantage of multi-path fading of wireless channels. For simple implementation and low cost, multiple antennas are usually placed at an AP while mobile nodes (MNs) are equipped only with one omni-directional antenna. As a result, by utilizing the multiple antennas at the AP, the AP-bottleneck can be smoothed.

1.1 Overview of Previous Work

Much research has been conducted on the performance analysis of IEEE 802.11b/a MAC based on both error-free and error-prone channels. The behavior of the IEEE 802.11 Distributed Coordination Function (DCF) protocol has been extensively studied in the literature [2, 3, 4] based on error-free channels. The work in [2] is assumed a saturation case in which every station always has a packet to transmit; however, the maximum channel throughput can be achieved only with non-saturated case [3]. The saturation throughput in a Gaussian wireless error channel has also been studied in [5, 6, 7], while a few papers have studied the WLAN throughput under wireless fading channels [8, 9]. Our interest in

this thesis is to extend the model in [3] for Rayleigh fading channels.

Due to the impact of Rayleigh fading channel, the existing WLANs have a very limited performance in terms of data rate in which the demand of high performance wireless networks has increased in the recent years. Thus, the next generation IEEE 802.11n has been proposed to provide up to 600 Mbps [10] considering PHY and MAC enhancement. In order to efficiently enhance the MAC throughput for the IEEE 802.11n WLAN, various frame aggregation schemes have been proposed in [11, 12].

Currently, the potential data rate extension for high-speed WLANs is based on a combination of MIMO with orthogonal frequency division multiplexing (OFDM) [13, 14]. Basically, the tremendous throughput improvement can be achieved by exploring the capacity of smart antenna systems over fading channels. A lot of research efforts have been carried out to exploit the capacity of single-user transmission where there are multiple antennas at both transmitter and receiver [15, 16, 17]. However, in the infrastructure WLAN, it may not be suitable to have multiple antennas at an MN because of limitation on size, battery power and cost. As a result, the study of multi-user transmissions, in which the AP equipped with multiple antennas and a group of receivers each with single antenna, has emerged. In [18, 1], the downlink capacity region of multi-user transmissions has been investigated based on assumptions such as a sufficient pre-coding techniques at the transmitter and perfect channel state information at the transmitter.

1.2 Objectives

The main objective of this thesis is to study the MAC performance in terms of network capacity and throughput by using smart antenna over Rayleigh fading channels. Although there are a few papers studying the WLAN performance over wireless fading channels, to the best of our knowledge, none of them jointly considers the MAC performance and the underlying smart antenna technologies used in multi-path fading channels. In this thesis, an analytical model is developed to study the performance of 802.11 MAC over flat-fading channel. The capacity and throughput of the IEEE 802.11n WLAN can be obtained considering diversity and multiplexing gains. As the AP serves one user at a time, we explore how the WLAN performance is affected by the data rate enhancement in the uplink and downlink transmissions under the diversity gain of multiple antennas employed in the AP. When the AP serves multiple users simultaneously in the downlink, the potential throughput is investigated by considering the multiplexing gain of multiple antennas.

1.3 Thesis Outline

The remainder of the thesis is organized as follows. An overview of the IEEE 802.11 PHY and MAC protocols is presented in Chapters 2. Chapter 3 gives a brief background about smart antenna systems. The analytical model is developed in Chapter 4, followed by numerical results in Chapter 5. Finally, Chapter 6 provides conclusions and further research directions.

Chapter 2

Wireless Local Area Networks

Wireless local area networks (WLANs) have become very popular due to low cost, easy deployment, and Internet access. First, we present a general overview of WLAN standards in section 2.1. WLAN architecture is presented in section 2.2. Finally, a brief description about the physical and MAC layers are presented in section 2.3 and 2.4, respectively.

2.1 General Overview

Recently, WLANs have received considerable attention because they efficiently join data connectivity and mobility over a limited geographical area. WLANs consist of wireless devices equipped with wireless cards using radio frequency to exchange data. Two main standards are commonly used for WLAN: the high performance radio local area network (HiperLAN) [19], which is proposed by the European Telecommunications Standards Institute (ETSI) and the 802.11, which is proposed by IEEE [20]. The standards aim to define a

set of rules (protocols) to provide a technique for multiple vendors to operate in systematic way over radio frequency bands. These rules cover both the physical (PHY) layer and the medium access control (MAC) layer of the open systems interconnection (OSI) reference model. Currently, the most frequently used standard is the IEEE 802.11, also known as Wi-Fi.

In 1996, the first version of the HiperLAN/1 was developed and issued by the Broadband Radio Access Networks (BRAN) project. The scope of the HiperLAN is to develop higher data rate than IEEE 802.11. The link layer is divided into MAC and channel access control (CAC) sub-layers, in which Elimination-Yield Non-Preemptive Multiple Access mechanism (EY-NPMA) is adopted to support priority and accessing policy. Then, the second version HiperLAN/2 is proposed to provide QoS, integration with high-speed networks (e.g. 3G mobile core networks and Asynchronous Transfer Mode (ATM)) and some level of security.

In 1997, the IEEE 802.11 was released by working group (WG) as the first WLAN standard. The goal of the IEEE 802.11 is to develop a MAC and PHY specification in order to provide wireless communications for different types of users (e.g. fixed or mobile) within a local area. There are two types of services, asynchronous data transfer, which is specified by mandatory support, and distributed time-bounded services (DTBS), which is specified by optional support [21]. Therefore, the IEEE 802.11 defines two MAC modes to sustain both services, the mandatory distributed coordination function (DCF) and the optional point coordination function (PCF). On the one hand, the DCF provides a fair accessing mechanism to the network, and it is designed for asynchronous data transfer. On the other hand, the PCF is based on polling schemes to provide a degree of priority for real time traffic.

IEEE 802.11b was ratified in 1999. It supports up to 11 Mbps data rate by extending the DSSS modulation technique in the original standard. Employing the promising OFDM technique, IEEE 802.11a/g further improve the data rate to 54 Mbps. The dramatic increase in the data rate and substantial price reductions lead to the rapid deployment of IEEE 802.11 WLANs. In addition, there exist a number of standards related to several tasks: security (i.e. 802.11i), functionality (i.e. providing QoS, increasing data rate such as IEEE 802.11e and 802.11n, respectively) and integration (i.e. 802.11s). The PHY and MAC layers play an important role to develop these standards according to users' demands. In section 2.3 and 2.4, we will describe more about each layer.

2.2 WLAN Architecture

The standard building block in the IEEE 802.11 is called the basic service set (BSS), which consists of a group of two or more stations that communicate with each other. Based on transmission fashion and the existing of a centralized controller, the 802.11 characterizes two main network topologies: the ad-hoc and the infrastructure-based networks. First, the ad-hoc network, also known as independent BSS (IBSS) is a BSS without a centralized access point (AP) and each station can communicate with other stations in a peer-to-peer fashion as shown in Figure 2.1. Second, the infrastructure network consists of at least an AP, and a distributed system (DS). All stations within BSS communicate with their AP in client-server fashion, so all frames between stations must go through the AP, where an AP communicates with another AP through the DS. A set of infrastructure BSS's, where the access points communicate amongst themselves through the DS, is defined as an extended

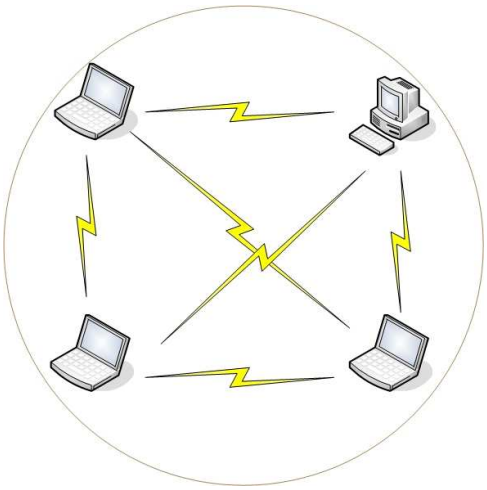

Figure 2.1: Independent basic service set (IBSS)

service set (ESS) as shown in Figure 2.2.

2.3 The Physical Layer

The physical layer is divided into two components: the Physical Layer Convergence Procedure (PLCP) performs some additional PHY-dependent framing before transmission, while the Physical Medium Dependent (PMD) layer is responsible for the actual transmission rates. The IEEE 802.11 defines three physical techniques for WLANs: infrared light (IR), frequency hopping spread spectrum (FH or FHSS) and direct sequence spread spectrum (DS or DSSS). While the infrared technique operates at the baseband, both FHSS and DSSS operate at the license-free 2.4 GHz Industrial, Scientific, and Medical (ISM) band (i.e. 2.4 - 2.4835 GHz). As shown in Figure 2.3, IEEE 802.11 defines a single MAC over four different physical layers [22].

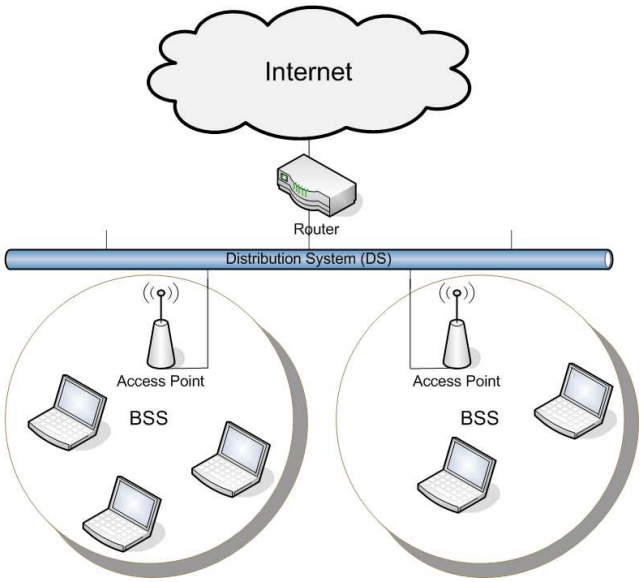

Figure 2.2: Extended service set (ESS)

- High-Rate Direct Sequence (HR/DS or HR/DSSS) used in 802.11b
- Orthogonal Frequency Division Multiplexing (OFDM) used in 802.11a
- Extended Rate PHY (ERP) used in 802.11g
- MIMO used in 802.11n

In 802.11b, the supported transmission rates are 1 Mbps, 2 Mbps, 5.5 Mbps and 11 Mbps. As the transmission rate at 1 Mbps uses differential binary phase shift keying (DBPSK), which encodes one bit per symbol. The transmission rate at 2 Mbps uses a four-level encoding mechanism, two bits per symbol, called differential quadrature phase shift keying (DQPSK). Based on complementary code keying (CCK), the 5.5 Mbps is achieved by encoding four bits per symbol while the maximum 11 Mbps requires encoding

<table>
<tr><td colspan="4">IEEE 802.2
Logical Link Control (LLC)</td><td rowspan="2">Data Link Layer</td></tr>
<tr><td colspan="4">IEEE 802.11 (CSMA/CA)
Medium Access Control (MAC)</td></tr>
<tr><td>HR/DSSS</td><td>OFDM</td><td>ERP-OFDM</td><td>MIMO-OFDM</td><td>PHY layer</td></tr>
<tr><td>802.11b</td><td>802.11a</td><td>802.11g</td><td>802.11n</td><td>802.11 Standards</td></tr>
</table>

Figure 2.3: IEEE 802.11 standards mapped to the OSI reference model

eight bits per symbol [23].

Due to huge traffics in the 2.4 GHz ISM band, the 802.11a move to the license-free 5 GHz band to provide higher data rate at the price of sacrificing transmission range and power. The 802.11a PHY adopts the orthogonal frequency division multiplexing (OFDM) technique. The basic ideal behind the OFDM technique is to break high-speed data carrier into several lower-speed sub-carriers to be transmitted in a parallel manner. Basically, the physical layer uses a symbol rate of 250,000 symbols per second, and each frequency carrier in the 5 GHz band, which is 20 MHz wide, is composed of 52 sub-carriers, each 300 KHz wide. In 802.11a, 48 sub-carriers are used for data while the remaining four sub-carriers are considered as pilot carriers for controlling issues. There are eight different transmission rates depending on different modulation schemes such as binary phase shift keying (BPSK), quadrature phase shift keying (QPSK) and quadrature amplitude modulation (16-QAM and 64-QAM). For the lower supported rates 6 and 9 Mbps, BPSK is used to encode 1 bit per sub-carrier or 48 bits per symbol. While the convolutional coding uses either half or one quarter of the bits as redundant bits for error correction, there are only 24 or 36

data bits per symbol. So the achievable data rate using BPSK is (24 or 36) times 250,000 equaling 6 or 9 Mbps. Similarly, when 802.11a uses QPSK, 16-QAM and 64-QAM to encode 2 bits, 4 bits, 6 bits per sub-carrier, the achievable data rate enhances to 18, 36, 54 Mbps, respectively [24].

To address backwards compatibility with the installed base of 802.11b, 802.11g is standardized to offer high data rate and operate in the 2.4 GHz band. The 802.11g adopts several physical layer specifications under a name of Extended Rate PHY (ERP). ERP-CCK is backwards compatible with 802.11b while ERP-OFDM is the main part of 802.11g to achieve the high data rate of 802.11a [25].

The need for higher data rates in WLANs boosts drastically because of huge consumer interest in multimedia applications. Over the past few years, the potential growth of data rate has noticeably climbed from 1 Mbps to 54 Mbps. Currently, 802.11 Task Group n (TGn) is in the process of standardizing the next-generation WLAN technology aiming to provide up to 100 Mbps at the medium access control (MAC) service access point (SAP). The design of the next-generation WLAN requires advance wireless communications to improve the physical transmission rate at least up to 200 Mbps [10]. The design of physical layer is based on multiple-input multiple-output (MIMO) and orthogonal frequency-division multiplexing (OFDM). Currently, both IEEE 802.11a and IEEE 802.11g are based on orthogonal frequency division multiplexing (OFDM) although a potential high data rate extension of these standards could be based on MIMO. As WLANs are usually deployed in indoor environments, which are typically characterized by a richly scattered multi-path, MIMO takes advantage of the multi-path environments and leads to a potential capacity increment. Thus, MIMO systems improve the channel capacity

significantly by adopting multiple transmit and receive antennas [13]. Beside increasing the channel capacity, MIMO resists the fading condition and reduces power consumption. Basically, time-varying wireless fading channels cause variations in the received signal-to-noise ratio (SNR), which also cause the variations in the bit error rate (BER). For lower SNR, the modulation scheme faces difficulties to decode the received signal. The more complex modulation scheme such as QAM is, the higher SNR is required. Unfortunately, every increase in data rate is usually achieved through the use of a complex modulation, which requires a high SNR. The solution to obtain significant higher data rates without increasing SNR is using MIMO technique at the physical layer, so in this thesis we will investigate the potential capacity of the IEEE 802.11n MIMO.

2.4 The Medium Access Control Layer

As collisions waste a lot of bandwidth and network capacity, the IEEE 802.11 DCF uses a carrier sense multiple access/collisions avoidance (CSMA/CA) with a binary exponential backoff rather than the collision detection, which is used by Ethernet [20]. Access to the wireless channel is controlled by CSMA/CA to reduce the collision probability. DCF defines two access mechanisms: Basic access and Request To Send/Clear To Send (RTS/CTS) access mechanisms. The IEEE 802.11 PCF requires centralized controller (i.e. AP) to provide contention-free service and QoS to some real-time applications. In this thesis, we will focus on the CSMA/CA basic access mechanism.

To implement CSMA and CA, two types of carrier-sensing mechanisms, the physical carrier-sensing and virtual carrier-sensing, combine together. While the physical carrier-

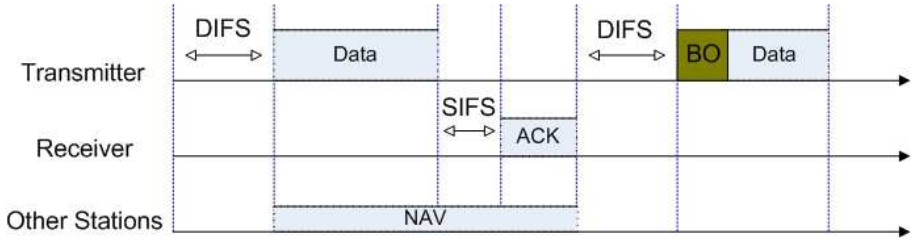

Figure 2.4: CSMA/CA basic access mechanism

sensing discovers whether the channel is busy or not through a clear channel assessment function, the virtual carrier-sensing is optionally provided by the network allocation vector (NAV). When any station is ready to transmit a frame, it must monitor the channel before attempting to transmit. If the channel is sensed busy, the station must defer until the channel is sensed idle for an interval of time equal to a distributed interframe space (DIFS). Then, the STA goes into a random backoff time in which it sets a uniformly random number from the interval [0, CW-1], where CW is called the contention window size. For each unsuccessful transmission, the value of CW is doubled until reaching a maximum value called CWmax; then, it resets to a minimum value called CWmin when the frame is dropped or after a successful transmission. The backoff time is decremented by one every idle slot, otherwise it is frozen. It resumes again after the medium is sensed idle for a DIFS. The station can transmit when the backoff time reaches zero, and the other stations hearing the transmission defer their transmissions by adjusting their NAVs. If the frame is received successfully, an acknowledgement (ACK) is transmitted after a short interframe space (SIFS) by the receiver. In DCF, if a transmitter does not receive an ACK, it retransmits the frame and increases its CW size. The CSMA/CA basic access mechanism is shown in Figure 2.4.

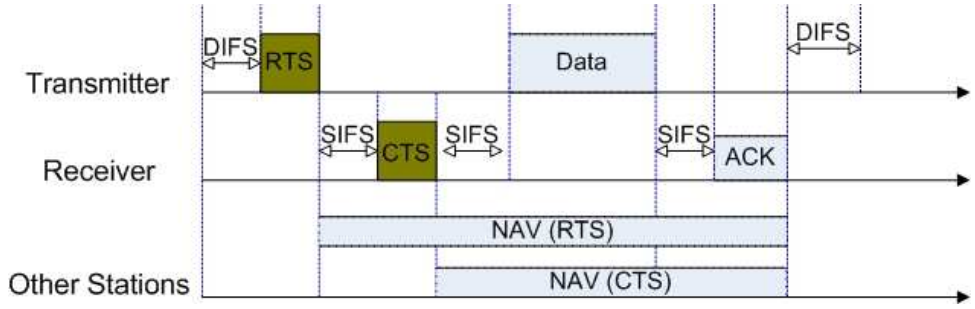

Figure 2.5: CSMA/CA RTS/CTS mechanism

Unfortunately, the 802.11 standard cannot distinguish collisions from transmission errors at the MAC layer, so it handles both of them as a transmission failure. Transmission failure could occur due to collisions or transmission errors. Collisions may occur when two or more stations start transmissions simultaneously while transmission errors may occur due to the channel conditions such as fading, path loss, etc.

To deal with the hidden terminal problem, an optional four way hand-shaking technique, known as the CSMA/CA RTS/CTS mechanism, is introduced. Before a station attempts to transmit a frame, the transmitter sends a short RTS frame, 20 bytes, and the receiver replies with a CTS frame, 14 bytes, if it is ready to receive. Once the transmitter receives the CTS frame, it transmits the data frame. Other stations hearing an RTS update their NAVs with the duration of the data frame transmission. Figure 2.5 shows the RTS/CTS mechanism.

Chapter 3

Wireless Communications and Smart Antenna Technologies

Next-generation WLAN uses advanced wireless communication systems to overcome some exiting challenges, e.g., the limited radio spectrum and time-varying wireless fading channels. Smart antenna techniques have been proposed to meet the increasing demand for higher data rate, QoS and mobility. Recently, multiple antenna systems are considered to be a breakthrough in wireless communication that exploits space dimension to improve wireless systems capacity, range and reliability. In this chapter, we will give a brief introduction about wireless channels in section 3.1. The statistical model for fading channels that we used in the thesis is presented in section 3.2. Then, we study the diversity and multiplexing gains of multiple antenna systems in section 3.3.

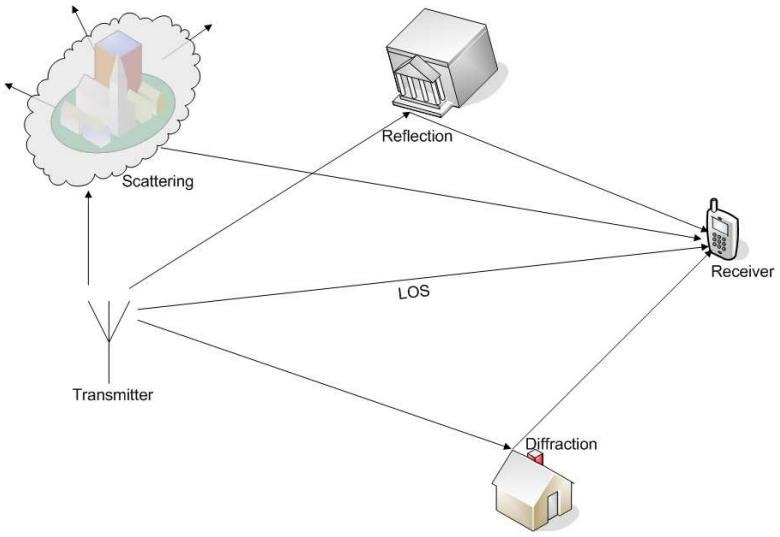

Figure 3.1: Different paths in wireless channels

3.1 Wireless Channels

In wireless systems, as a mobile receiver moves, multiple delayed versions of transmitted signal may arrive at the receiver along different paths due to several factors, e.g. scattering, diffraction and reflection. As shown in Figure 3.1, if there is no obstacle between the transmitter and receiver, a line of sight (LOS) channel carries the strongest and dominant signal to a receiver while others may reach the receiver at different time instants due to reflection caused by buildings, trees or other obstacles. Generally, reflections via sharp surface are known as diffraction and via several small objects are known as scattering.

The reduction of received signal power is due to two main impairments: the large-scale effect, and the small-scale effect. As a result, the received signal power is given by

$$P_r = P_t - L(d) + X + Y(t), \tag{3.1}$$

where P_t, P_r are the transmitted and received signal power respectively, $L(d)[dB]$ is the path loss which is the reduction of transmitted signal power caused by distance d, $X[dB]$ is a Gaussian random variable representing the shadowing effects $Y(t)$ is a random process representing the fading effects. The following sections describe more about these effects.

3.1.1 Large-Scale Effect

Large-scale effect is the average signal power attenuation due to motion over large area and can be classified into two components: path loss and shadowing. Basically, the variation in mean received signal strength as a function of distance is known as large-scale effect and is described as follows [26]

$$L(d) = L(d_0) - 10v \log_{10}(\frac{d}{d_0}) + X[dB], \tag{3.2}$$

where $L(d)$ and $L(d_0)$ are path loss in dB at distance d and d_0 respectively, v is a path loss exponent and $X[dB]$ is the shadowing. First, path loss, also known as attenuation, can be defined as *the reduction of power density of an electromagnetic wave as it propagates through space*. Path loss may occur due to many factors such as propagation losses, refraction, diffraction, reflection, height and location of antennas, etc. In fact, path loss is a heavily dependent environment in which the path loss exponent varies from 2 to 6. The average received power decreases proportionally with distance between the transmitter and receiver ($P_r \propto d^{-v}$). The path loss by itself (without considering shadowing)can be modeled as follows [26]

$$L(d) = L(d_0) - 10v \log_{10}(\frac{d}{d_0}). \tag{3.3}$$

Second, shadowing is random variations in received signal strength due to geometries of the paths between the transmitter and receiver. For a given distance d, the signal power may vary due to obstructions such as hills or large buildings. The shadowing is modeled as a log-normal distribution, and the probability density function (PDF) of x in dB is a Gaussian random variable with zero mean and standard deviation σ as follows

$$f(x) = \frac{1}{\sqrt{2\pi}\sigma} \exp(-\frac{x^2}{2\sigma^2}). \tag{3.4}$$

3.1.2 Small-Scale Effect

Fading is caused by multi-path propagation between the transmitter and receiver, which results from the constructive and destructive combination of multi-paths. Due to multi-path properties, each path may experience a different attenuation, time delay and phase shift. Multi-path propagation results in the spreading of the signal in two different dimensions, delay spread and Doppler spread. Delay spread is the time difference between the arrival time of first path and the last one due to receiving the same signal at different times.

Based on delay spread, the fading channels can be classified into two types: frequency-flat and frequency-selective fading channels. When the coherence bandwidth is greater than the signal bandwidth, the channel is considered as a frequency-flat fading channel. However, in frequency-selective fading channels, the coherence bandwidth is less than the signal bandwidth, which causes intersymbol interference (ISI). Hence, the received signal might be lost.

Based on Doppler spread, the fading channels can be classified into two types: slow (time-flat) and fast(time-selective) fading. In slow fading, a low Doppler spread occurs

when the coherence time is greater than the symbol period and the channel impulse response variations are slower than the transmitted baseband signal variations. On the other hand, the fast fading has a high Doppler spread in which the coherence time is less than the symbol period, and the channel impulse response variations are faster than the transmitted baseband signal variations [26].

In summary, there are four main factors that influence the short-term fading: multi-path propagation, motion of mobile nodes, motion of surrounding objects, and transmission rate of the signal. The fading channels can be classified into four types: frequency-flat slow fading, frequency-flat fast fading, frequency-selective slow fading and frequency-selective fast fading. In literature, several statistical models are proposed to study the behavior of the amplitude and phase of the received signal power. According to a slow mobility in WLAN, we consider the frequency-flat slow fading channel, also known as a quasi-static Rayleigh fading channel. Therefore, we will study a Rayleigh fading model in the following section.

3.2 Rayleigh Fading Channels

The nature of the amplitude multi-path channel is random due to the random location of objects in the environment. Rayleigh fading is most applicable when there is no LOS between the transmitter and receiver, while Rician fading is used when there is a LOS. The Rayleigh fading channel satisfies two conditions: the number of multiple paths (N) between the transmitter and receiver is large, and there is no LOS path. Thus, the received

signal $r(t)$ is a summation of all N random paths plus a Gaussian noise as follows [26]

$$\begin{aligned} r(t) &= \sum_{i=1}^{N} a_i(t)\cos(2\pi f_c t + \theta_i(t)) + n(t) \\ &= x(t)\cdot\cos(2\pi f_c t) - y(t)\cdot\sin(2\pi f_c t) + n(t), \end{aligned} \tag{3.5}$$

where f_c is the carrier frequency, $n(t)$ is the Gaussian noise, $a_i(t)$ and $\theta_i(t)$ are the amplitude and phase of the ith component, respectively, and $x(t) = \sum_{i=1}^{N} a_i(t)\cos(\theta_i(t))$ and $y(t) = \sum_{i=1}^{N} a_i(t)\sin(\theta_i(t))$ are random processes representing the summation of N random paths. For large N, using the central limit theorem, both $x(t)$ and $y(t)$ are approximated as independent identically distributed (iid) Gaussian random processes with zero mean and variance σ^2. To characterize the channel, the fading channel gain can be defined as follows:

$$h(t) = x(t) + jy(t) = a(t)\exp(j\theta(t)), \tag{3.6}$$

where $h(t)$ is the fading channel gain, $a(t)$ and $\theta(t)$ are the amplitude and phase of the fading channel, respectively. The fading channel gain has two parameters:

1. Fading amplitude is represented by the envelope of the received signal ($R = \sqrt{x^2 + y^2}$) which follows a Rayleigh distribution as follows

$$f_R(r) = \frac{r}{\sigma^2}\exp(-\frac{r^2}{2\sigma^2}). \tag{3.7}$$

.

2. fading phase follows a uniform distribution given by

$$f_{\phi}(\phi) = \frac{1}{2\pi}. \tag{3.8}$$

Given the transmitted signal $s(t)$, the received signal $r(t)$ is given by

$$r(t) = h(t)s(t) + n(t). \tag{3.9}$$

As known, the channel capacity is the maximum data rate that a channel can support with asymptotically small error probability. In 1948, Cluade Shannon derived the channel capacity for additive white Gaussian noise (AWGN) channels under the assumption that the signal power is bounded and the Gaussian noise process is characterized by a power spectral density as follows [27]

$$C = B \cdot (\log_2(1 + SNR)), \tag{3.10}$$

where B is the bandwidth of the channel in hertz, C is the channel capacity in bits per second and $SNR = \frac{P_{signal}}{P_{noise}}$ is the signal-to-noise ratio. In practice; however, Shannon capacity is not achieved because coding techniques should be applied to overcome the channel errors. Basically, coding techniques reduce the transmission rate to achieve a certain level of error probability at a receiver. Thus, as coding techniques improve, Shannon capacity limit is approached more closely.

In addition to white Gaussian noise, the wireless channels are under other impairments as mentioned in section 3.1, which reduce the channel capacity significantly and can be

described as follows [28]

$$C = B \cdot (\log_2(1 + SNR \cdot |h|^2)), \tag{3.11}$$

where $|h|^2$ is the average normalized fading channel gain. For deep fading conditions, the channel capacity degrades significantly. The capacity in Equation 3.11 depends on [16]

1. Channel Distribution Information (CDI) which is defined by whether the distribution of h is known to the transmitter and receiver or not.

2. Channel State Information (CSI) which is defined by whether the value of instantaneous channel gain h is known to the transmitter and receiver or not.

For time-varying channel, the channel capacity relies on what is know about CDI and CSI at the transmitter and/or receiver. There are two scenarios of channel capacity based on the randomness of the channel gain:

- Ergodic capacity (Ergodic Shannon capacity): While the channel gain is drawn randomly, the channel capacity depends on the distribution and value of the channel gain as follows

$$\begin{aligned} C &= B \cdot E_h(\log_2[1 + SNR \cdot |h|^2]) \\ &= B \cdot \int \log_2[1 + SNR \cdot |h|^2] p(h) dh, \end{aligned} \tag{3.12}$$

  where $p(h)$ is the PDF for the channel gain.

- Non-ergodic channel (outage capacity): At the beginning of transmission, the channel gain is drawn randomly and then stays fixed for the rest of the transmission.

3.3 Diversity and Multiplexing Gains

To improve channel capacity and link reliability of next-generation wireless systems, multiple antenna systems should be employed at both the transmitter and receiver. However, the design of efficient modulation and coding scheme to achieve these goals is a challenging issue. Multiple input multiple output (MIMO) systems introduce two important techniques: diversity and multiplexing. On the one hand, multiple antennas have been used to combat channel fading and increase diversity. While there exists different paths between the transmitter and receiver, sending signals that carry the same information through different paths, provides multiple independently faded replicas of the transmitted data at the receiver end. Hence, the reception reliability is enhanced. Spatial multiplexing, on the other hand, is an approach to transmit independent data streams in parallel fashion through different transmit antennas; therefore, the data rate is increased. In practical systems, there is a traditional tradeoff between transmission rate and probability of errors which leads to the same tradeoff between spatial multiplexing and diversity [29]. The following sections describe more about these techniques and their tradeoff.

3.3.1 Diversity Gain

In Gaussian channels, channel coding techniques are proposed to reduce probability of errors in wireless channels caused by the statistically independent errors (i.e. additive white Gaussian noise (AWGN)). These coding techniques add some redundancy into the transmitted data to allow a receiver to detect or correct the errors. Unlike the Gaussian channel, the wireless channel suffers from several other impairments such as the path loss,

the shadowing and the fading which may result in a large number of errors. Therefore, diversity approach can be used to improve system performance in terms of link reliability. For example, in a slow Rayleigh-fading environment with one transmit antenna and N receive antennas, the maximal diversity gain is equal to N in which the average probability of error can be decreased to $\frac{1}{SNR^N}$ instead of $\frac{1}{SNR}$ in single antenna case [17]. There are three kinds of diversity techniques which are commonly used in wireless communication systems:

- Time (Temporal) Diversity is to transmit the desired signal in different time slots separated by more than the coherence time of the channel. To efficiently exploit time diversity, both channel coding and time interleaving are used. Thus, copies of the transmitted signal are provided to the receiver in the form of redundancy in temporal domain.

- Frequency Diversity is to transmit the copies of the desired signal in different frequency carriers, where each frequency carrier is separated by more than the coherence bandwidth of the channel. Thus, copies of the transmitted signal are provided to the receiver in the form of redundancy in the frequency domain. However, frequency diversity is not bandwidth efficient and it needs to tune to different frequency carriers at both transmitter and receiver.

- Spatial (Antenna) Diversity uses multiple antennas separated by more than half of a wavelength. Obviously, the use of multiple antennas is not suitable and difficult for small devices (i.e., mobile handset and laptop) due to the size and battery power limitation. Therefore, it is more desirable to adopt multiple antennas at the base

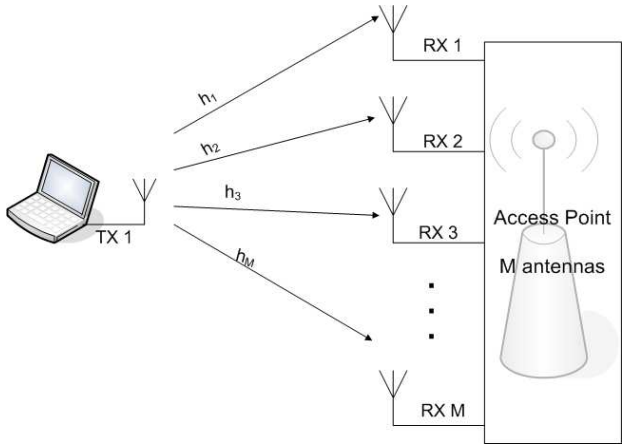

Figure 3.2: Receiver diversity

station. Thus, the copies of transmitted signal are provided to the receiver in the form of redundancy in spatial domain[30]. Spatial diversity can be classified into three types: receiver diversity, transmit diversity and mixture diversity.

- Receiver diversity is achieved for uplink transmissions (single-input multiple-output SIMO channels) as shown in Figure 3.2. At the receiver, the replicas of these transmitted signals can be combined to reduce the amplitude variations caused by fading channels. There are two main combining schemes: maximum ratio combining (MRC) and selection combining (SC). MRC is an optimum matched filter in which received signals are added together, but SC chooses the received signal with the highest SNR. The maximum diversity order, which depends on the number of independent fading paths, is equal to the number of receive antennas.
- Transmit diversity is achieved for downlink transmissions (multiple-input single-

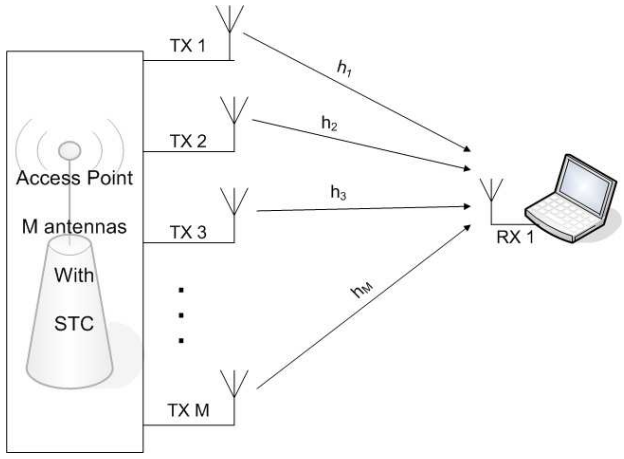

Figure 3.3: Transmit diversity

output MISO channels) as shown in Figure 3.3. Transmit diversity relies on two challenging tasks, designing the transmitted signal and knowing a channel state information at transmitter (close-loop or open-loop transmit diversity). These tasks assign additional complexity and pre-processing at the transmitter. Space-time coding is an open-loop transmit diversity technique, and it is considered to be the key technique for exploiting the spatial diversity. Basically, STC can be classified into two classes, space-time trellis codes (STTC) and space-time block codes (STBC). The maximum diversity order, which depends on the number of independent fading paths, is equal to the number of transmit antennas.

– Combination of the receive and transmit diversity is achieved for MIMO channels. The maximum diversity order, which depends on the number of independent fading paths, is equal to the product of the number of transmit and receive antennas.

3.3.2 Multiplexing Gain

In addition to achieving diversity, multiple antenna systems are capable to increase the capacity which results in a high transmission rate. Spatial multiplexing is an approach where the transmitted data is divided into multiple sub-streams in which each sub-stream is transmitted on a different transmit antenna. In a rich scattering environment, the receiver can separate the data streams, and the capacity increases by a maximum spatial multiplexing order, which is the minimum of the number of transmit and receive antennas. Recently, some researchers have focused on exploring the capacity of single-user transmission where multiple antennas at both the transmitter and receiver such as Bell Laboratories Layered Space-Time (BLAST) [15] . However, other researchers have proposed a possibility of multi-user transmissions. The capacity of multi-user MIMO channel is classified into two basic channels, the MIMO multiple-access channel (MAC) for uplink and the MIMO broadcast channel (BC) for downlink as shown in Figure 3.4 [31].

We are interested in the multi-user downlink channel where multiple antennas at an access point (AP) can serve multi-users simultaneously in the downlink which results in a capacity enhancement proportional to the number of antennas at the AP and the number of users. Generally, the multiple antennas at the AP for downlink transmissions have been extensively studied in the PHY layer for maximizing the multiplexing gain [1, 32, 18]. To support multiple users simultaneously in the downlink transmissions, pre-coding techniques at the AP are required to eliminate multi-user interference and divide the wireless channel into multiple independent single-input single-output (SISO). Pre-coding techniques can be classified into two categorizes, non-linear and linear pre-coding. The non-linear pre-coding (e.g. Dirty Paper Coding (DPC)) achieves the maximum capacity, but its complexity makes

Table 3.1: Comparison between linear and non-linear pre-coding [1]

Pre-coding	Non-linear	Linear
Example	DPC	Beamforming Zero-forcing
After pre-coding (x)	$x = v_1 s_1 \oplus (v_2 s2 \oplus ...)$	$x = \sum_{i=1}^{k} v_i s_i$
Throughput	Maximum	Degradation because of rate offset
Optimality	Optimal	Sub-optimal
Complexity	High	Low
Channel equivalents	K-SISO parallel channels	1-MIMO channel

*: where $\oplus$ is non-linear operation, x is the transmitted signal, v_i is the precoding matrix, and s_i is original signal

it non-practical in real systems. On the other hand, linear pre-coding can achieve almost the same multiplexing gain at a lower complexity. But linear pre-coding may result in a rate/power offset[1]. Table 3.1 summarizes the differences between linear and non-linear pre-coding. Thus, multiple antennas are becoming popular in next generation technologies such as IEEE 802.11n because they improve the transmission rate significantly.

3.3.3 Diversity-Multiplexing Tradeoff

Multiple antennas can be used for improving the link reliability via diversity gain, or for improving the transmission rate via multiplexing gain. This fundamental tradeoff exists in all communication systems between the transmission rate (multiplexing) and probability of error (diversity). Obviously, an increase in SNR for fixed transmission rate will reduce the probability of error, but an increase in SNR for fixed probability of error will increase transmission rate [31]. In fact, approaching higher diversity order results in sacrificing spatial multiplexing. In [17], the authors propose a scheme that can achieve a fundamental tradeoff between diversity and multiplexing. The optimal diversity gain can be obtained

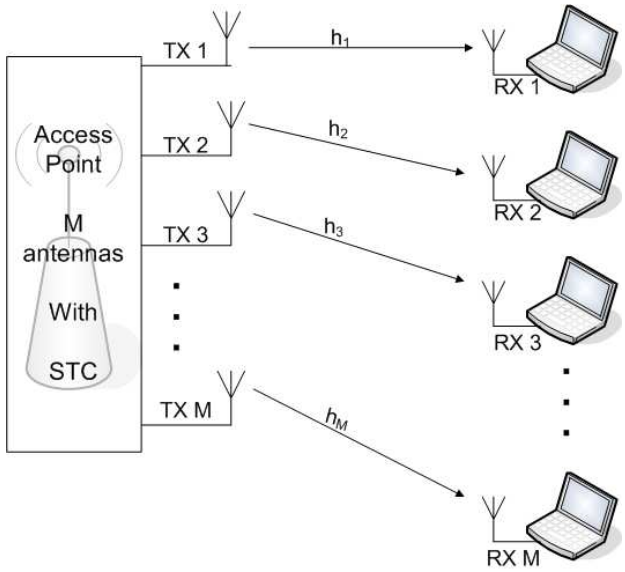

Figure 3.4: Multi-user uplink/downlink channels

from as follows [17]

$$d^*(r) = (m - r)(n - r), \tag{3.13}$$

where $d^*(r)$ is a diversity order as a function of multiplexing gain r, and m,n are the transmit and receive antennas, respectively. Equation 3.13 suggests that while r transmit and receive antennas are used for multiplexing, the remaining $m - r$ and $n - r$ are used for diversity. Therefore, when multiplexing gain r equals to maximum value, which is $min(m, n)$, the value of diversity order goes to zero. Similarly, if the multiplexing gain r equals to zero, the diversity gain $d^*(r)$ equals to maximum value mn. Otherwise, the channel can simultaneously achieve both gains.

Chapter 4

Analytical Model

In this chapter, we present an analytical model of the IEEE 802.11 DCF protocol using smart antenna techniques over Rayleigh fading channels. In section 4.1, we study the capacity of flat Rayleigh fading channels for various system architectures such as SIMO, MISO and MIMO. Then, the analytical model that analyzes the behavior of 802.11 MAC over flat-fading channel is presented in section 4.2. Considering the diversity gain of multiple antennas employed in the AP, we study the capacity of the WLAN for single user transmission in section 4.3. In section 4.4, we investigate the potential throughput of the IEEE 802.11n WLAN via the multiplexing gain of multiple antennas.

4.1 Capacity of Flat Rayleigh Fading Channels

The characteristics of the indoor propagation channel at 2.4 GHz is investigated in [33]. Most of WLANs are deployed in indoor environments which are usually characterized by

a richly scattered multi-path [13]. The performance of WLANs degrades significantly in terms of channel capacity due to the multi-path fading in wireless channels. As a result, the existing standards such as IEEE 802.11 a/b/g work to reduce the effects of multi-path fading. In the next generation WLANs, multiple antenna systems have a great potential to achieve high throughput by taking advantage of multi-path fading channels. However, multiple antennas are usually placed at an AP because it is very likely that mobile nodes (MNs) be equipped only with an omni-directional antenna for simple implementation and low cost.

In this thesis, we consider two different scenarios, a SIMO/MISO system that can be used for single-user transmission and a virtual MIMO system that can be used for multi-user transmissions. A SIMO/MISO system consists of multiple antennas at the AP and single omni-antenna at a MN, while a virtual MIMO system consists of multiple antennas at AP and multiple MNs each with single omni-antenna. Interestingly, we explore the absolute gains offered by multiple antennas by studying the channel capacity limit of SIMO, MISO and MIMO [34, 35]. According to a slow mobility in WLAN, we consider the flat slow fading channel, also known as a quasi-static slow Rayleigh fading channel, and the channel gain is the average of Rayleigh fading channels. The channel state information at transmitter (CSIT) plays an important role to maximize the channel capacity in MISO and MIMO systems, but it is difficult to be obtained. However, channel state information at receiver can be obtained through the transmission of a training sequence [36].

4.1.1 Capacity of SIMO Flat Rayleigh Fading Channels

Single input multiple output (SIMO) systems have a single antenna at the transmitter and multiple antennas at the receiver. While SIMO system includes only a single transmit antenna, the CSIT provides no capacity increase. Thus, the capacity can be derived as follows

$$C_{SIMO} = B \cdot (\log_2(1 + SNR \cdot \sum_{i=1}^{M_R} |h_i|^2)), \tag{4.1}$$

where M_R is the number of receive antennas and $\sum_{i=1}^{M_R} |h_i|^2$ is the summation of channel gains for all receive antennas. Practically, the theoretical limit of data rate of an IEEE 802.11a/g WLAN with bandwidth $B = 16\ MHz$ is 133 $Mbps$. The currently achievable data rate in a practical WLAN is far below that limit due to the implementation of the underlying modulation and coding techniques. Therefore, we use a coefficient η to denote the coding and modulation efficiency in the MAC layer. For example, for the IEEE 802.11g WLAN where $C_{AWGN} = 133\ Mbps$, we have $\eta = 0.4$ and the achieved data rate is $54Mbps$ [37]. Thus, the achievable data rate (R_{SIMO}) can be simplified as follows

$$R_{SIMO} = \eta \cdot B \cdot [\log_2(1 + M_R \cdot H_{avg} \cdot SNR)], \tag{4.2}$$

where H_{avg} is the average normalized complex channel gain of Rayleigh fading channel. Therefore, by using multiple receive antennas, the capacity increases with the number of receive antennas; this increment of SNR is known by array gain. Figure 4.1 shows the capacity of SIMO system considering $H_{avg} = 1$.

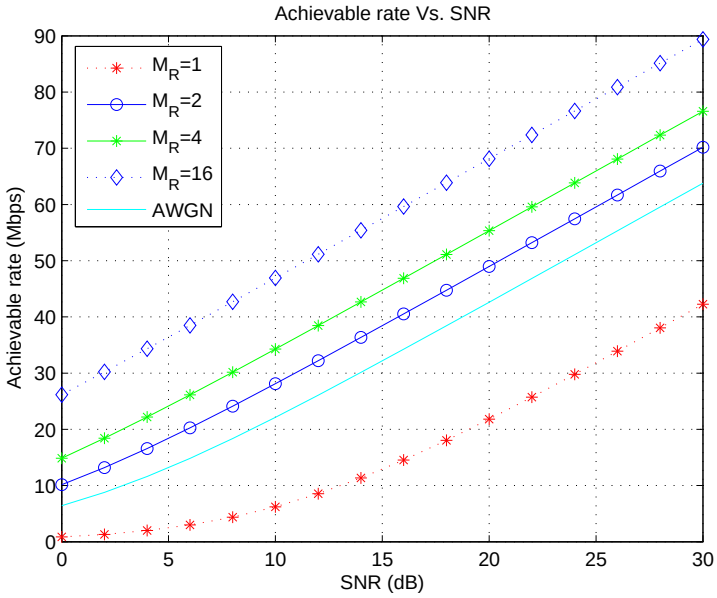

Figure 4.1: Achievable rate of SIMO flat-Rayleigh fading channels

4.1.2 Capacity of MISO Flat Rayleigh Fading Channels

Multiple input single output (MISO) systems have multiple antennas at the transmitter and single antenna at the receiver. When the transmitter does not have the CSI, the transmission power is divided into all the transmit antennas (M_T); hence, the capacity is given by

$$C_{MISO} = B \cdot (\log_2(1 + \frac{SNR}{M_T} \cdot \sum_{i=1}^{M_T} |h_i|^2)), \tag{4.3}$$

where M_T is the number of transmit antennas and $\sum_{i=1}^{M_T} |h_i|^2$ is the summation of channel gains for all transmit antennas. In Equation 4.3, while the power is divided into M_T transmit antennas, the maximum value of MISO capacity approaches the ideal AWGN channel with single antenna at both the transmitter and receiver. Then, the achievable

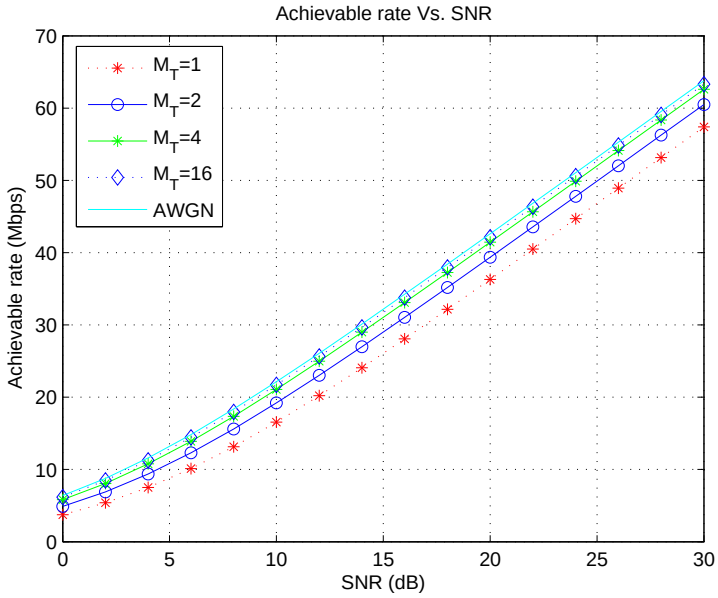

Figure 4.2: Achievable rate of MISO flat-Rayleigh fading channels

data rate (R_{MISO}) is given by

$$R_{MISO} = \eta \cdot [B \cdot (\log_2(1 + \frac{SNR}{M_T} \cdot \sum_{i=1}^{M_T} |h_i|^2))]. \tag{4.4}$$

Figure 4.2 shows that the transmit diversity is able to remove the effect of fading for a large number of antennas. However, the MISO capacity equals the SIMO capacity when the CSI is known at transmitter [35].

4.1.3 Capacity of MIMO Flat Rayleigh Fading Channels

Multiple input multiple output (MIMO) systems have multiple antennas at both the transmitter and receiver. While the CSI is completely unknown at the transmitter, the trans-

mitted power is divided equally likely into M_T transmit antennas. Then, the capacity is given by

$$C_{MIMO} = B \cdot (\log_2 det[I_{min(M_T,M_R)} + \frac{SNR}{M_T} \cdot H \cdot H^H]), \tag{4.5}$$

where $I_{min(M_T,M_R)}$ is the identity matrix. The capacity of the channel depends on the channel matrix gain (H) and its conjugate (H^H) as follows

$$H = \begin{bmatrix} h_{1,1} & h_{1,2} & \dots & h_{1,M_T} \\ h_{2,1} & h_{2,2} & \dots & h_{2,M_T} \\ \vdots & \vdots & \ddots & \vdots \\ h_{M_R,1} & h_{M_R,2} & \dots & h_{M_R,M_T} \end{bmatrix}, \tag{4.6}$$

where $h_{i,j}$ represents the channel gain between the $\imath th$ MN and the $\jmath th$ antenna at the AP. By applying pre-coding technique at the AP for downlink transmission, the downlink channel is decomposed into multiple parallel independent sub-channels to maximize the channel capacity [38]. Therefore, the achievable data rate increases linearly with the number of transmit antennas as follows [35].

$$R_{MIMO} = M \cdot \eta \cdot [B \cdot (\log_2(1 + SNR * H_{avg}))], \tag{4.7}$$

where $M = min(M_R, M_T)$. Figure 4.3 shows the linear increment in capacity proportional to the number of transmit antennas at AP. However, if the CSI is known to both transmitter and receiver, the transmitted power will be adjusted according to water-filling algorithm in order to maximize the mutual information which is out of scope of this thesis [39, 40].

In summary, we study the flat Rayleigh fading channel capacity of three channel con-

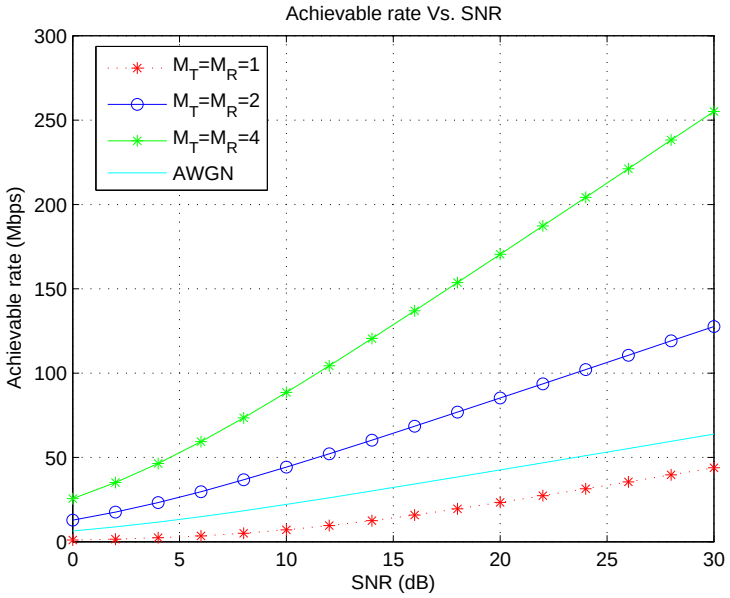

Figure 4.3: Achievable rate of MIMO flat-Rayleigh fading channels

figurations SIMO, MISO, and MIMO. In single-user transmission for unknown CSIT, the capacity of SIMO is much higher than the capacity of MISO, so the system performance can be improved in terms of higher data rate in uplink, but the high traffic load at the AP makes the AP the system bottleneck. Therefore, we consider a perfect CSIT in which the capacity of both SIMO and MISO are the same to improve the over all system performance for the uplink and downlink. Then, we will introduce multi-user transmissions by fully utilizing the multiple antennas at the AP via multiplexing gain to improve the system performance.

4.2 Extended Analytical Model for Rayleigh Fading Channel

The performance of IEEE 802.11a/b/g WLAN has been extensively studied in the literature, mainly based on an error-free channel condition [2, 3, 4]. The aim of these research works is to derive suitable analytical models to study the performance of DCF 802.11 protocols in saturated and non-saturated cases. However, most of the previous work focuses on the MAC performance in an ideal physical channel. The saturation throughput in a Gaussian wireless error channel has also been studied in [5, 6, 7]. Although the wireless channel suffers from several other impairments such as, the path loss, shadowing and multi-path fading, researchers usually use the Gaussian channel due to its simplicity. Moreover, there are a few papers study the WLAN throughput under wireless fading channels [8, 9].

In this section, first, we begin by extending the analytical model in [3] for Rayleigh fading channels. Second, we obtain the system throughput based on a realistic case in which the AP is saturated and the MNs are non-saturated to explore the maximum throughput of the system.

As shown in Figure 4.4, the system model consists of an AP with multiple antennas, and N-1 mobile nodes (MNs), all employing a single omni-directional antenna. The transmission failures in the system may occur due to either frame collisions caused by two or more stations transmit at the same time or frame corruptions caused by deep fading channel conditions. Some reasonable assumptions are:

- A multi-path Rayleigh fading channel;

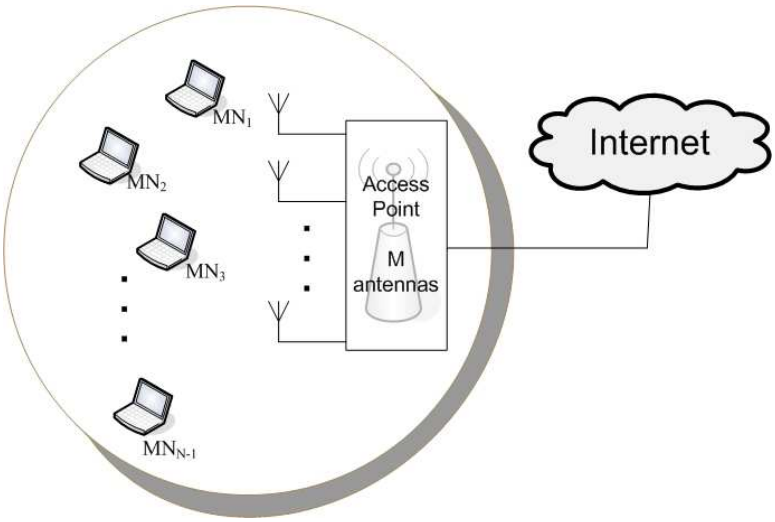

Figure 4.4: System model

- Perfect CSI at both the transmitter and receiver;
- We consider collisions are due to two stations transmitting simultaneously since the probability of three or more stations simultaneously transmitting is very small;
- All mobile nodes (MNs) have the same traffic arrival rate, frame service rate and frame size.

Table 4.1 summarizes all notations used in the thesis.

4.2.1 Mathematical Model

First, the probability of a transmission failure of an MN is given by

$$P_f = 1 - (1 - P_c)(1 - P_e) = P_c + P_e + P_c P_e, \tag{4.8}$$

Table 4.1: List of symbols

N	Number of mobile nodes (MNs)	M	Number of antennas
λ	The average arrival rate (frame/slot)	R_i	Achievable data rate for system i
μ	The average service rate (frame/slot)	H_{avg}	The average channel gain
ρ	The queue utilization ratio	SNR	The average signal-to noise ratio (dB)
η	Modulation and coding coefficient	B	The channel bandwidth (Hz)
P_c	Probability of collision	$E[W]$	Average backoff time
P_f	Probability of transmission failure	L_{Data}	Payload length of data frame
τ	Probability of transmission	L_{ack}	Payload length of ACK frame
P_e	Probability of frame error	T_s	Time duration of successful transmission
P_e^{data}	Probability of data frame error	T_f	Time duration of failure transmission
P_e^{ack}	Probability of ACK frame error	P_b	Bit error rate (BER)

where P_c is the collision probability and P_e is the error probability. Errors may occur on either data frames with probability P_e^{data} or ACK frames with probability P_e^{ack}. Since data or ACK frames are transmitted independently, the total probability of error is given by

$$P_e = P_e^{data} + (1 - P_e^{data})P_e^{ack} = P_e^{data} + P_e^{ack} - P_e^{data}P_e^{ack}. \tag{4.9}$$

The error probability P_e is affected by the frame length; hence, P_e^{data} and P_e^{ack} are given by

$$P_e^{data} = 1 - (1 - P_b)^{L_{data}} \tag{4.10}$$

$$P_e^{ack} = 1 - (1 - P_b)^{L_{ack}}, \tag{4.11}$$

where P_b is the probability of bit error rate (BER) of a wireless channel depending on SNR and the modulation scheme [41]. The collision probability is determined by the number of

contending stations,

$$P_c = 1 - (1 - \rho\tau)^{N-1}, \tag{4.12}$$

where $\rho = \frac{\lambda}{\mu}$ is a traffic intensity of a station, and τ is the transmission probability. Thus, we rewrite the probability of failure P_f in Equation 4.8 as follows

$$P_f = 1 - (1 - \rho\tau)^{N-1}(1 - P_e). \tag{4.13}$$

Finally, the service rate is given by

$$\frac{1}{\mu} = [(N-1)\rho + 1]T_s + \frac{1}{2}[(N-1)\rho + 1]T_f \cdot \frac{P_f}{1 - P_f} + E[W], \tag{4.14}$$

where both τ and $E[W]$ are functions of P_f instead of only P_c as in [3]. In the basic access mechanism, T_s and T_f are determined by the achievable data rate in the channel as follows

$$T_s = T_f = 2 * T_{PHYheader} + \frac{(L_{data} + L_{ACK})}{R_i} + T_{DIFS} + T_{SIFS}, \tag{4.15}$$

where $T_{PHYheader}$ is the time to transmit the physical layer overheads consisting of PLCP and Preamble headers, and R_i is the achievable data rate of an i system. For example, the SISO achievable data rate is given by

$$R_i = R_{SISO} = \eta[B \cdot (\log_2(1 + SNR \cdot H_{avg}))]. \tag{4.16}$$

For given values of N, λ and H_{avg}, we obtain the failure probability P_f and the frame service rate μ by numerically solving Equations 4.13 and 4.14.

In an infrastructure WLAN, we have two different traffic arrival rates for the AP and the MNs which are denoted as λ_{AP} and λ_{MN}, respectively; also the service rates of the AP and the MNs are denoted as μ_{AP} and μ_{MN}. Similarly, all other parameters of the system such as P_f and $E[W]$ can be classified into two types for the AP and the MNs as follows:

$$\begin{cases} P_f^{AP} = 1 - (1 - \rho_{MN}\tau_{MN})^{N-1}(1 - P_e^{AP}) \\ \\ P_f^{MN} = 1 - (1 - \rho_{MN}\tau_{MN})^{N-2}(1 - \rho_{AP}\tau_{AP})(1 - P_e^{MN}) \end{cases} \tag{4.17}$$

$$\begin{cases} \frac{1}{\mu_{AP}} = \left((N-1)\frac{\lambda_{MN}}{\mu_{AP}}T_s^{up} + T_s^{down} + \frac{1}{2}(N-1)\frac{\lambda_{MN}}{\mu_{AP}}\overline{T_f^{up}} + \frac{1}{2}\overline{T_f^{down}}\right) + E[W_{AP}] \\ \\ \frac{1}{\mu_{MN}} = ((N-2)\rho_{MN} + 1)T_s^{up} + \frac{\lambda_{AP}}{\mu_{MN}}T_s^{down} + \frac{1}{2}((N-2)\rho_{MN} + 1)\overline{T_f^{up}} + \frac{1}{2}\frac{\lambda_{AP}}{\mu_{MN}}\overline{T_f^{down}} + E[W_{MN}], \end{cases} \tag{4.18}$$

where $\overline{T_f^{up}} = T_f \cdot \frac{P_f^{MN}}{1-P_f^{MN}}$ and $\overline{T_f^{down}} = T_f \cdot \frac{P_f^{AP}}{1-P_f^{AP}}$ are the average failure time of a transmitted frame for uplink and downlink transmission, respectively. As mentioned before, the successful and failure transmission time depends on the achievable data rate. For instance, in SISO system, the uplink and downlink have symmetrical achievable rate given by Equation 4.16. Then, we substitute Equation 4.16 in Equation 4.15 to compute both the successful and failure transmission time for uplink and downlink. The Equations 4.17 and 4.18 can be solved numerically to compute P_f^{AP}, P_f^{MN}, μ_{AP} and μ_{MN}. Obviously, the arrival rate of the AP is much larger than the arrival rate of MN, as all traffics to and from the WLAN have to go through the AP, which makes the AP the system bottleneck. Then, the maximum number of flow connection in the WLAN can be determined by the queue

utilization ratio of the AP ($\rho_{AP} \leq 1$).

4.2.2 System Throughput

To compute the system throughput, we consider a saturated AP where ρ_{AP} equals to one while the MNs are non-saturated. The downlink throughput equals to the frame service time of the AP (μ_{AP}) multiply by the frame payload (L_{AP}), while the throughput of non-saturated MNs equals to $(N-1) * \lambda_{MN} * L_{MN}$. Thus, the system throughput is given by

$$S = \mu_{AP} * L_{AP} + (N-1) * \lambda_{MN} * L_{MN}, \tag{4.19}$$

where S is the system throughput, L_{AP}, L_{MN}, and λ_{MN} are given, and μ_{AP} can be calculated from Equations 4.17 and 4.18.

4.3 Diversity Gain of Multiple Antennas

Although the signal power drops significantly due to multi-path fading channels, extensive research has shown that antenna diversity can effectively improve the performance of WLANs [42, 43, 44]. While [42] presents the throughput analysis considering antenna diversity at the AP, [43, 44] focus on the physical layer analysis. However, we study the MAC performance of an IEEE 802.11n WLAN considering the capacity enhancement provided by antenna diversity at AP.

Antenna diversity is described by an access point using multiple antennas to transmit/receive signals to/from a single-antenna mobile station. Thus, the AP explores the

diversity gain of multiple antennas by two methods. First, receiver diversity is achieved for the uplink SIMO system. Second, transmit diversity is achieved for the downlink MISO system. By exploring the diversity gain of multiple antennas, the reliability of the link increases up to maximum diversity gain M. In addition to increasing link reliability, we are interested in the capacity enhancement as mentioned in Section 4.1. Based on a perfect CSIT, SIMO and MISO provide the same capacity enhancement [35], so the uplink and downlink have symmetrical achievable rate given by Equation 4.2. By substituting Equation 4.2 in Equation 4.15, the successful and failure time are reduced as follows

$$T_s = T_f = 2 * T_{PHYheader} + \frac{(L_{data} + L_{ACK})}{R_{SIMO}} + T_{DIFS} + T_{SIFS}. \tag{4.20}$$

Hence, the performance of WLAN is slightly improved. However, the maximum multiplexing gain equals to $min(M, 1) = 1$, so there is no multiplexing gain [17].

4.4 Multiplexing Gain of Multiple Antennas

In conventional 802.11, only a single-user transmission can be supported at a time which means a transmission occurs either from an AP to a MN or from a MN to an AP. However, AP with multiple antennas can communicate with multiple users simultaneously by using pre-coding techniques at the AP. This technique is known as space-division multiple access (SDMA). Basically, the downlink channel between an AP with multiple antennas and a group of MNs with single antenna can be described as a virtual MIMO channel, while the uplink channel can be described as SIMO channel. We are interested in the MIMO

downlink channel in order to smoothen the bottleneck at the AP. The MIMO downlink channel is heavily dependent on the channel knowledge at the transmitter. While CSI can be obtained at the receiver using training, CSI at the transmitter requires a feedback from each MN [45, 16]. The capacity region for downlink channel with perfect CSI at both transmitter and receiver has been extensively studied in [18, 32, 1]. Based on a coding strategy called "writing on dirty paper" [46], Caire and Shamai [18] have proposed the sum capacity of a broadcast channel with two antennas at the transmitter and two receivers each equipped with a single antenna. Then, [32] extends the Caire-Shamai region to multiple users and multiple receive antennas. Based on these studies, we present a simplified capacity derivation for MIMO downlink channel.

In our model, the AP can serve random different users simultaneously without any significant modification in the MAC protocol. The AP senses the medium and transmits to multiple users simultaneously when the medium is sensed idle as follows

$$Y = Hs + n, \tag{4.21}$$

where $Y = [y_1 y_2 ... y_M]^T$ is the received signals for the downlink, $s = [s_1 s_2 ... s_M]^T$ is the transmitted signals, $n = [n_1 n_2 ... n_M]^T$ is the additive independent complex Gaussian noise with unit variance, and H is the channel matrix gain as in Equation 4.6. We assume an independent identical distributed (iid) frequency-flat Rayleigh fading channel and perfect CSI at both the AP and all MNs. By using sufficient pre-coding technique (i.e. DPC or linear pre-coding [1]) at the AP, the multi-user interference will be eliminated and the downlink channel will be divided into M SISO independent channels as shown in Figure

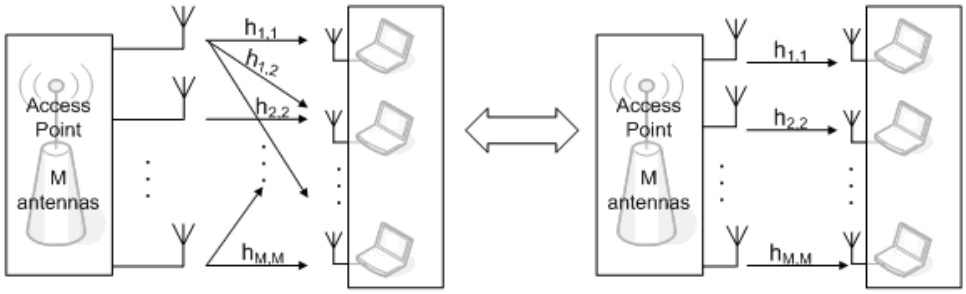

Figure 4.5: Downlink channel for multi-user transmission

4.5. As a result, each antenna at the AP transmits to one user over an SISO channel. The transmission time (either successful or failure) for each antenna in the downlink channel is given by

$$T_i = 2 * T_{PHYheader} + \frac{(L_i^{data} + L_{ACK})}{R_{SISO}} + T_{DIFS} + T_{SIFS}, \tag{4.22}$$

where T_i is the transmission time that the antenna i takes to transmit L_i^{data} to user i in the downlink. Since the AP serves different users simultaneously over SISO channels, the transmission time T_i in the downlink is similar to SISO case and given by Equation 4.15. However, the service rate of the AP is given by ($\mu_{AP} = M \cdot \mu_i$) which results in reducing the traffic intensity at the AP as follows

$$\rho_{AP} = \frac{\lambda_{AP}}{\mu_{AP}} = \frac{\lambda_{AP}}{M \cdot \mu_i}, \tag{4.23}$$

where μ_i is the service rate of antenna i. For ACK frames in the uplink, the channel is classified as MIMO multiple-access channel (MAC) as mentioned in Chapter 3. In MIMO MAC channel, the collision between nodes is a challenging issue [31]. For simplicity, in this thesis we consider collision-free channel for ACK frames in the uplink.

For non-saturated MNs, when many users have been served by the AP, they may not contend the channel immediately resulting in greatly reduction of collisions in the WLAN. Therefore, the collision probability will be reduced comparing to SISO system because the AP serves multiple users simultaneously which leads to decrease the MN's contention. However, when the number of user increases in the WLAN, the contention increases as well. In our model, the downlink collision may occur between M frames from the AP and other frames from MNs. Intuitively, the collision loss in the downlink channel severely degrades the WLAN performance because the collision may occur to more than $M + 1$ frames.

In uplink transmission scenario, the MN transmits the frame over a SIMO channel and the transmission time is giving by Equation 4.20. Finally, by substituting Equations 4.15 and 4.20 in Equation 4.18, and Equation 4.23 in Equation 4.17, Equations 4.17 and 4.18 can be solved numerically to compute P_f^{AP}, P_f^{MN}, μ_{AP}, and μ_{MN}.

Chapter 5

Numerical Results

In this chapter, we study the system performance in terms of capacity and throughput by using the analytical model for SISO, SIMO and MIMO systems. Section 5.1 introduces the system parameters and traffic model used in the analytical model. The effect of Rayleigh fading channel in SISO system is presented in section 5.2. In single user transmission, we study the effect of the slightly capacity enhancement of a SIMO system in section 5.3. In section 5.4, we investigate the potential improvement of data rate for the promising IEEE 802.11n WLAN considering multiplexing gain of multiple antennas.

5.1 Experiment Setup

To evaluate the performance of the analytical model, the IEEE 802.11a is used and the main parameters are given in Table 5.1. The data rate equals to 54 *Mbps* in an error-free channel. Due to Rayleigh fading channels, the achievable data rate of the channel decreases

Table 5.1: The IEEE 802.11a parameters

T_{DIFS} (μs)	34	PLCP & Preamble (μs)	24
T_{SIFS} (μs)	16	SNR (dB)	25
Slot Time (μs)	9	MAC Header (Byte)	34
CW_{min}	16	RTP/UDP/IP Headers	40

and consequence, MAC-header, RTP/UDP/IP-headers, ACK and data frames will take longer time to transmit. For example, if the channel gain equals to 0.08, the achievable rate reduces from 54 $Mbps$ to 30.2 $Mbps$; hence, an ACK frame takes $14*8/30.2 = 3.7\mu s$ instead of $2.07\mu s$. Also, the MAC overhead takes $34 * 8/30.2 = 9\mu s$ and the RTP/UDP/IP-header takes $40*8/30.2 = 10.6\mu s$. Under multi-path fading channel, the reduction of the achievable rate is around 44%, which results in double the duration of frame transmission. Moreover, the throughput is limited at the MAC layer due to the higher MAC overhead. Increasing the throughput is strongly related to increase the transmission rate at the physical layer. In other words, the channel capacity needs to be enhanced to achieve higher transmission rate.

We consider two types of traffics: data and voice; however, the analytical model can support all kind of traffics. Data traffic is used with different frame size ($500 - 4500$ Bytes) and different average arrival rates. Generally, we choose the average arrival rate of MN equals 20 packets/sec and the payload length is 2000 bytes. While most of traffics go through the AP in WLAN, the average traffic load of the AP equals to $N - 1$ times the load of an MN. For voice traffic, we use $G.711$ codec which is an International Telecommunication Union (ITU) standard codec [47]. $G.711$ packetizes the signal into constant bit rate (CBR) at 64 $kbps$, and we consider 10 ms packetization interval results in 80 Byte payload length. We study the performance by considering a very bad multi-path fading

condition in which the average Rayleigh fading channel gain is 0.08. We use Maple 10 in our analysis [48].

5.2 SISO Fading Channel

We study the effect of Rayleigh fading channel in SISO system. Considering voice traffic, we compare the results with previous work in [3]. The throughput of data traffic is computed for different payload and number of MNs. Finally, the bottleneck of the AP is investigated under different fading conditions, in terms of the maximum number of flow connection and throughput.

Figure 5.1 shows the throughput of the AP and the system for different fading channels. We study the impact of payload length on the throughput under a fixed number of MN. The collision probability remains constant, while the error probability increases with the larger payload. Due to the characteristics of fading channel, as the channel experiences deeper fading condition, the channel capacity decreases and the error probability increases severely which leads to unstable AP. According to Equation 4.19, the AP-throughput depends on the service rate of the AP and the payload length. As shown in Figure 5.1, the throughput increases with the larger payload length; however, it begins to decrease after payload exceeds the certain threshold value in which the failure probability increases due to large number of errors and the frame service rate of the AP decreases. Although the AP throughput decreases rapidly, the system throughput decreases slowly because the MNs throughput increases with the number of active MNs for uplink transmission. Interestingly, large payload length degrades the throughput under a bad channel condition,

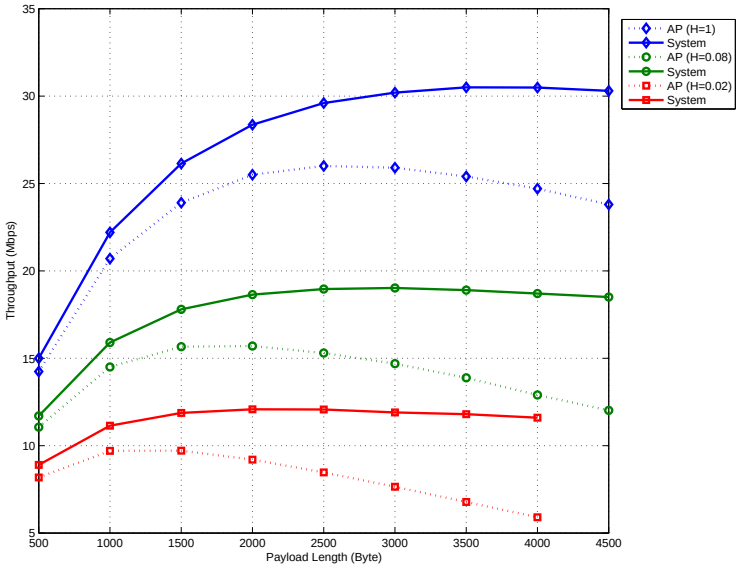

Figure 5.1: SISO throughput for different payload length

but it improves the throughput under a good channel condition.

On the other hand, with the increase number of flow connections, the throughput decreases due to the higher collision probability as shown in Figure 5.2. Thus, we can deduce that either a larger number of flow connections or a larger frame payload results in a higher failure probability; hence, the throughput degrades. In fact, bad fading channel causes significant degradation of the achievable data rate (according to Equation 4.16). The lower achievable data rate results in a longer time that a successful or failure transmission takes. Thus, the frame service rate reduces.

While the voice stream is modeled as a CBR traffic (without using the silence suppression), the arrival rate of an MN is constant and depends on the codec and the packetiztion

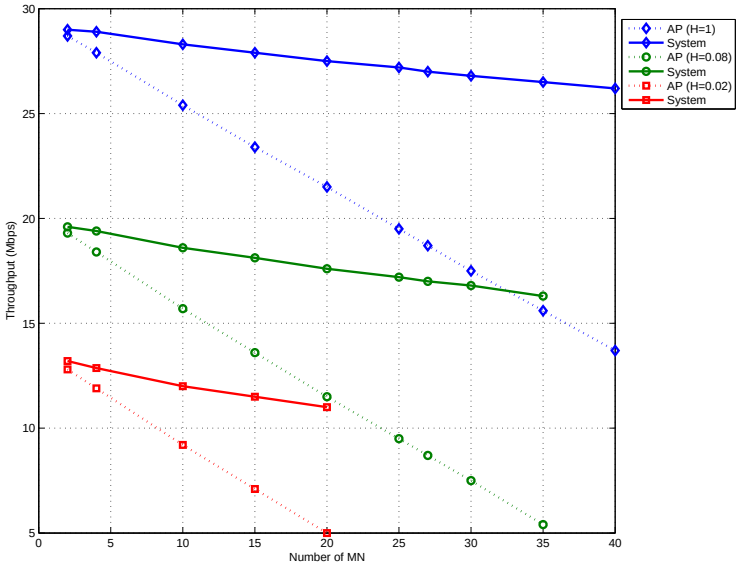

Figure 5.2: SISO throughput for different number of data Connections

interval; however, the arrival rate of the AP is $N-1$ times the arrival rate of MN because all the traffic goes through the AP as mentioned before. Consequently, a higher queue utilization ratio at the AP occurs with the increase of voice connections as shown in Figure 5.3. The erroneous channel increases the number of retransmission for corrupted frames which leads to increasing the load at the AP. The maximum number of voice connections reduces from 26 voice connections in a good channel condition to 20 voice connections due to bad Rayleigh fading channels. As a result, both the probability of errors and collisions increase the queue utilization at AP; hence, limit the number of maximum connection.

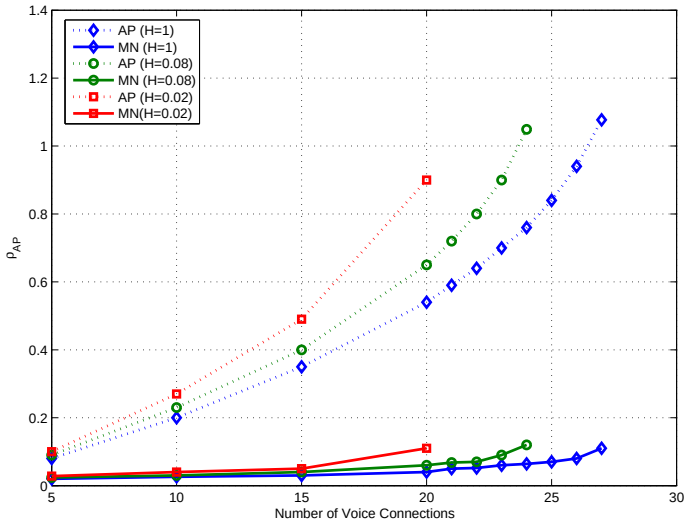

Figure 5.3: Queue utilization ratio of the AP and MNs for voice traffic

5.3 SIMO and MISO Fading Channel

In this section, we consider SIMO system in which multiple antennas at the AP and single antenna at each MN for single-user transmission. In SIMO system, the link reliability improves by maximizing the diversity gain, and the channel capacity enhances slightly with the increase number of antennas at the AP due to the array gain. We are interested in the capacity enhancement in SIMO. Therefore, we study the throughput and the maximum number of flow connections that can be supported in a single-AP WLAN.

Figure 5.4 shows the maximum number of MN that can be supported under different channel conditions. The worst channel condition results in a lower number of connections due to the higher error probability and capacity reduction. For single antenna at the AP, the number of connections drops by more than 50% due to the severe fading condition which

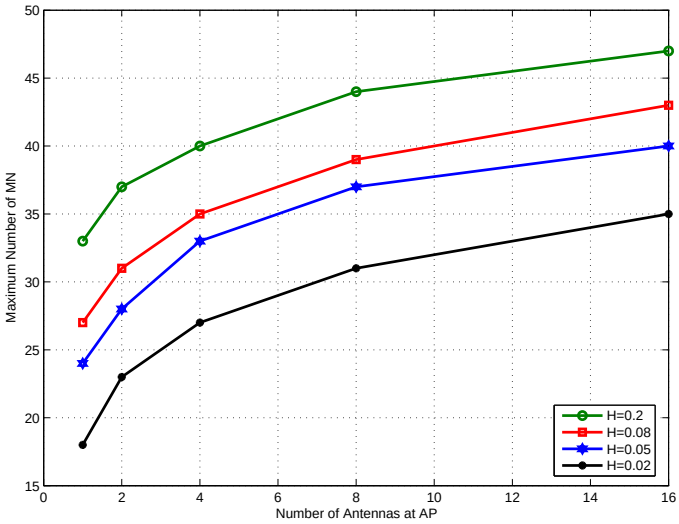

Figure 5.4: Maximum number of MNs in SIMO

causes a huge capacity reduction. For more than one antenna at the AP, the reliability of the link increases, so does the capacity. As shown in Figure 5.4, for example, when the number of antenna is eight comparing to one in a bad channel (i.e. $H = 0.02$), the improvement of the capacity is doubled. However, the maximum number of users is limited due to the higher collision probability for large number of user. Therefore, due to a little capacity improvement in SIMO, the maximum supportable stations are still limited even if we use large number of antennas.

The improvement of SIMO channel capacity shows a noticeable throughput growth comparing to SISO system. Figure 5.5 compares the system throughput of SIMO and SISO systems under various fading channels. By using fixed number of MNs and payload (i.e. $N = 10$ & $L = 2000Byte$), the four antennas at the AP reduces the harsh effect

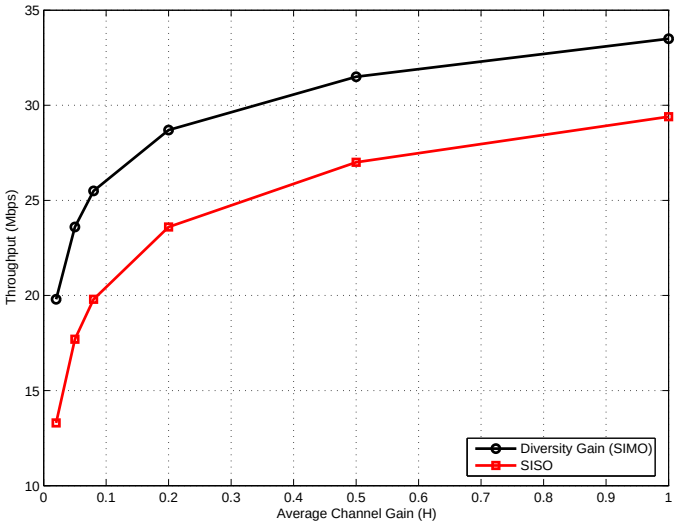

Figure 5.5: Throughput comparison between SIMO and SISO systems

of fading channel and improves the system throughput. Under bad channel condition (i.e. $H = 0.02$), the effect of four antennas is obvious and the throughput grows up from 13 $Mbps$ in SISO to 20 $Mbps$. On the other hand, when the channel is in a good condition, there is no significant improvement in terms of throughput. Therefore, while the total capacity enhancement in SIMO system is relatively small, we explore the significant capacity enhancement of multiple antennas by considering the multiplexing gain in the following section.

5.4 MIMO Fading Channel

In SISO fading channel, the IEEE 802.11 DCF model shows a significant degradation in system performance (e.g. 44% of the channel capacity). However, SIMO/MISO system focuses on reliability of the link in which the channel capacity improvement due to enhancing SNR is relatively small. So, we study the large capacity improvement using multiplexing gain of multiple antennas at the AP. We consider a possibility of serving multiple users simultaneously in the downlink channel by decomposing the channel into multiple parallel independent sub-channels. The sufficient pre-coding technique is employed at the AP to decompose the downlink channel. The downlink channel capacity increases linearly with the increase number of antennas. Therefore, the throughput of the IEEE 802.11n is investigated by exploring multiplexing gain of multiple antennas. The objective is to smoothen the AP-bottleneck and increase the total throughput of the WLAN.

Figure 5.6 shows the relationship between throughput and payload length for different number of antennas. For single antenna at the AP, bad Rayleigh fading channel causes severe channel capacity reduction which results in a low throughput. Adopting multiple antennas at the AP increases the channel capacity linearly and improves the throughput. When the number of antenna at the AP increases, the service rate of the AP increases which results in a high throughput. The significant improvement can be seen by using four antennas to serve four users at the same time. The presence of erroneous channel affects the throughput for large payload length.

For saturated AP, the maximum throughput is achieved at the lower number of MNs, and then it decreases with the increase number of MNs regarding to collisions as shown

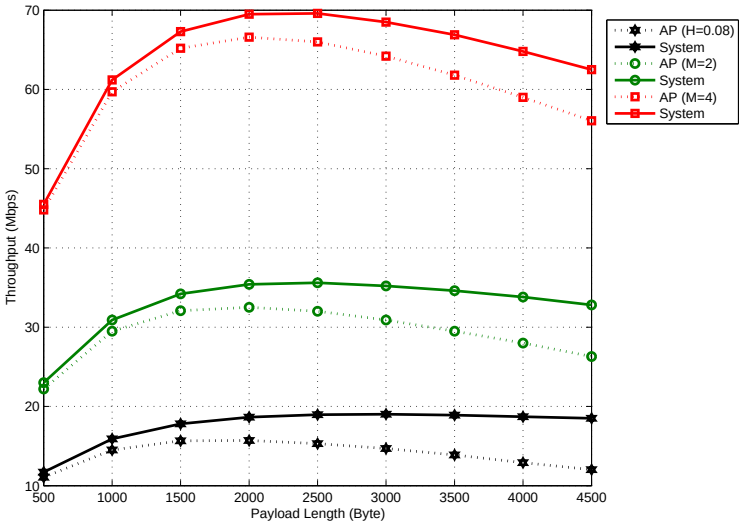

Figure 5.6: MIMO throughput for different payload length

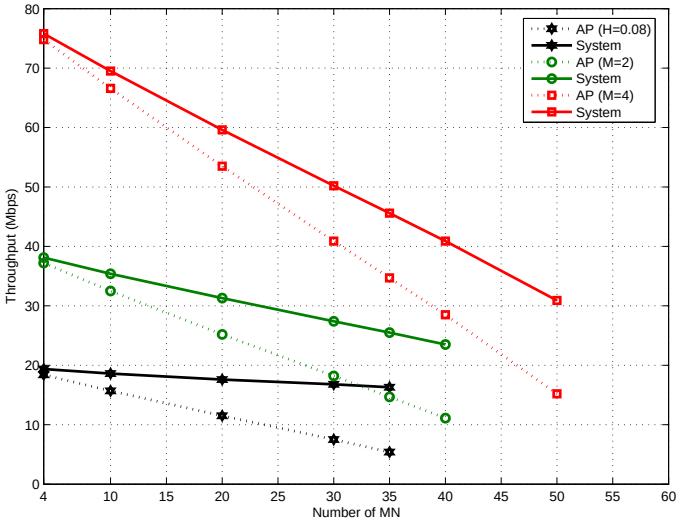

Figure 5.7: MIMO throughput for different number of data Connections

in Figure 5.7. In multiple antennas, as the number of MNs increases, the throughput of multiple antennas decreases sharply. This is because when a collision happens between the AP and MN in the downlink, all the collided frames (i.e. $M+1$ frames) are lost and need to be retransmitted. Thus, the collision probability rigorously increases.

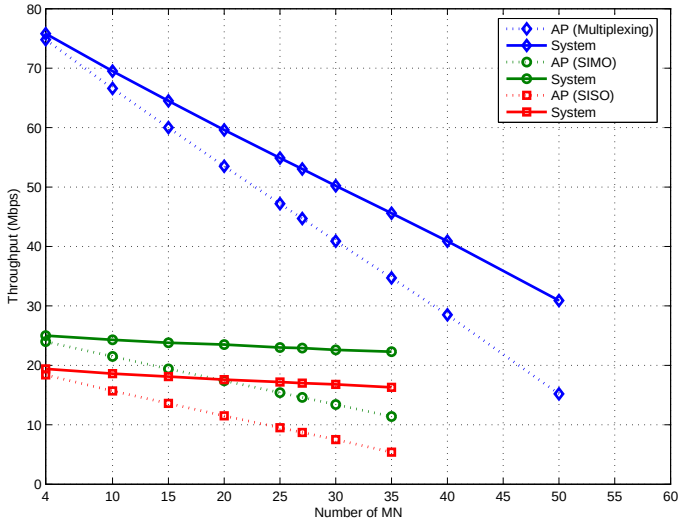

Figure 5.8: Throughput comparison among various systems

As discussed above, the downlink transmission has been improved by exploring the multiplexing gain of multiple antennas at the AP. Interestingly, Figure 5.8 compares the throughput of the three systems: SISO, SIMO and the multiplexing-AP with four antennas at the AP. The throughput of multiplexing-AP suffers from high collision probability when the number of user increases comparing to the other systems. The collision of $(M+1)$ frames causes a noticeable throughput degradation comparing to collisions of only 2 frames.

In conclusion, the channel capacity plays an important role to enhance the network

performance. Currently, SISO system suffers from both MAC overheads and PHY limitations. In next-generation WLAN, smart antenna systems can significantly improve the capacity channel by employing diversity and multiplexing gain. Based on serving one user at a time, the SIMO system overcomes the reduction in the channel capacity caused by multi-path fading. However, this improvement is relatively small in deep fading condition. The channel capacity of multiplexing-AP takes advantages of the multi-path fading properties and increases the channel capacity linearly. This chapter proves the advantage of using smart antenna in WLANs.

Chapter 6

Conclusion and Future Work

6.1 Conclusion

In this thesis, we have investigated the performance analysis of high-performance WLANs using smart antenna systems over Rayleigh fading channels. To the best of our knowledge, considering the MAC performance in cooperative with the underlying smart antenna technologies over Rayleigh fading channels is still lacking in literature. We have developed an analytical model to analyze the IEEE 802.11 DCF over multi-path fading channel.

The effect of Rayleigh fading channel humiliates the performance of SISO system because of the cruel reduction in the channel capacity. The results show a considerable AP-bottleneck which needs to be solved by smoothening the high load traffic. Consequently, adopting multiple antennas at the AP increases the channel capacity and smoothens the AP-bottleneck comparable to single antenna case. We have studied the potential of capacity improvement considering both multiplexing and diversity gain. Based on diversity

gain, SIMO provides slightly channel capacity enhancement which is enough to overcome the effect of fading channel but the AP-bottleneck is still there. We have addressed the AP-bottleneck through multi-user downlink transmissions in which the AP can serve M users simultaneously. To support multi-user downlink transmissions, pre-coding techniques (i.e. DPC) at the AP are required to eliminate multi-user interference and divide the wireless channel into multiple independent SISO channels. Therefore, significant throughput improvement is demonstrated by analyzing the multiplexing gain. However, the collision losses of multi-user downlink transmission have a significant impact on the system performance because the collision of $M + 1$ frames badly wastes the channel bandwidth as compared to a collision of only 2 frames. Finally, our results show the throughput increases linearly with the increase of the number of antennas. Hence, there is a significant improvement of system performance at the MAC layer by using smart antenna techniques.

6.2 Future Work

Although we have studied the performance of IEEE 802.11n by using a logical extension of the existing 802.11a standard, there are still several open issues:

- Link adaptation (LA) is essential to provide real-time streaming applications (i.e. HDTV) in the 802.11 WLANs. It is a process of dynamically selecting one of multiple available data transmission rates according to wireless link parameters such as transmission radio power, channel conditions and modulation/coding schemes. In our model, the quality of the wireless link is usually influenced by the Rayleigh fading channel conditions. Thus, the problem of radio link instability can be solved by

a sufficient LA scheme which needs further investigation.

- Supporting high definition video (HDV) and HDTV applications over WLAN is a challenging research topic. Further research on the capacity of HDTV over WLAN is vital to design Connection Admission Control (CAC) schemes in order to maintain the appropriate video quality.

- Addressing AP-bottleneck is a key issue in infrastructure WLANs. The heavily traffic at the AP can be further smoothed by using frame aggregation and bidirectional transmission. Consequently, the number of contentions and associated overheads at the AP will be reduced and the transmission efficiency improves. However, how large the concatenation frame at the AP should be is still a challenging optimization issue.

- QoS provisioning is also a key research issue in wireless networks. Since DCF is designed to support best effort traffic, the enhanced DCF (EDCF) and hybrid coordination function (HCF) are proposed in IEEE 802.11e [49] to provide service differentiation. EDCF provides priority to heavily load nodes such as the AP in our model. In addition to priority, the AP can be assigned a transmission opportunity (TXOP) in which the AP can send many frames as long as the duration of TXOP does not exceed the maximum duration of TXOP. Therefore, when the AP transmits M frames, the TXOP ensures the collision will never occur in the downlink.

- For a more realistic multi-user downlink transmission, the study of practical precoding techniques and obtaining a perfect CSI at both transmitter and receiver requires further exploration.

- In order to validate the results obtained by our analytical model, extensive simulation needs to be considered in our future work.

Bibliography

[1] J. Lee and N. Jindal. Dirty paper coding vs. linear precoding for MIMO broadcast channels. *Fortieth Asilomar Conference on Signals, Systems and Computers (ACSSC'06)*, pages 779–783, 2006.

[2] G. Bianchi. Performance analysis of the IEEE 802.11 distributed coordination function. *IEEE Journal on Selected Areas in Communications*, 18(3):535–547, March 2000.

[3] L. Cai, X. Shen, J.W. Mark, and Y. Xiao. Voice capacity analysis of WLAN with unbalanced traffic. *IEEE Transactions on Vehicular Technology*, 55(3):752–761, 2006.

[4] O. Tickoo and B. Sikdar. Queueing analysis and delay mitigation in IEEE 802.11 random access MAC based wireless networks. *INFOCOM Twenty-third AnnualJoint Conference of the IEEE Computer and Communications Societies*, 2, 2004.

[5] Q. Ni, T. Li, T. Turletti, and Y. Xiao. Saturation throughput analysis of error-prone 802.11 wireless networks. *Wiley Journal of Wireless Communications and Mobile Computing (JWCMC)*, 5:945–956, December 2005.

[6] J. Yin, X. Wang, and D.P. Agrawal. Optimal packet size in error-prone channel for IEEE 802.11 distributed coordination function. *Wireless Communications and Networking Conference (WCNC)*, 3:1654– 1659, March 2004.

[7] V. Vishnevsky and A. Lyakhov. 802.11 LANs: Saturation throughput in the presence of noise. *Proceedings of Networking*, 2345:1008–1019, 2004.

[8] Z. Hadzi-Velkov and B. Spasenovski. Saturation throughput-delay analysis of IEEE 802.11 DCF in fading channel. *IEEE ICC'03 International Conference on Communications*, 1, 2003.

[9] P.P. Pham. Comprehensive analysis of the IEEE 802.11. *Mobile Networks and Applications*, 10(5):691–703, 2005.

[10] Wi-Fi Certified. Wireless LAN Medium Access Control (MAC) and Physical Layer (PHY) specifications, longer-range, faster-throughput, multimedia-grade Wi-Fi networks, 2007.

[11] Y. Xiao. IEEE 802.11 n: enhancements for higher throughput in wireless LANs. *IEEE Wireless Communications*, 12(6):82–91, 2005.

[12] Y. Xiao. Efficient MAC strategies for the IEEE 802.11n wireless LANs. *Wireless Communications and Mobile Computing*, 2006.

[13] A.V. Zelst and T.C.W. Schenk. Implementation of a MIMO OFDM-based wireless LAN system. *IEEE Transactions on Signal Processing*, 52(2):483–494, 2004.

[14] S. Nanda, R. Walton, J. Ketchum, M. Wallace, and S. Howard. A high-performance MIMO OFDM wireless LAN. *IEEE Communications Magazine*, 43(2):101–109, 2005.

[15] G.J. Foschini. Layered space-time architecture for wireless communication in a fading environment when using multiple antennas. *Bell Labs Technical Journal*, 1(2):41–59, 1996.

[16] A. Goldsmith, SA Jafar, N. Jindal, and S. Vishwanath. Capacity limits of MIMO channels. *IEEE Journal on Selected Areas in Communications*, 21(5):684–702, 2003.

[17] L. Zheng and D.N.C. Tse. Diversity and multiplexing: a fundamental tradeoff in multiple-antenna channels. *IEEE Transactions on Information Theory*, 49(5):1073–1096, 2003.

[18] G. Caire and S. Shamai. On the achievable throughput of a multiantenna Gaussian broadcast channel. *IEEE Transactions on Information Theory*, 49(7):1691–1706, 2003.

[19] ETSI. Broadband radio access networks (BRAN); HIPERLAN type 2 technical specification; physical (PHY) layer. August 2000.

[20] IEEE standard 802.11. Wireless LAN Medium Access Control (MAC) and Physical layer (PHY) specifications, August 1999.

[21] B.P. Crow, I. Widjaja, L.G. Kim, and P.T. Sakai. IEEE 802.11 wireless local area networks. *IEEE Communications Magazine*, 35(9):116–126, 1997.

[22] G. Matthew. 802. 11 wireless networks: The definitive guide. *Sebastopol: O'Reilly*, 2005.

[23] IEEE standard 802.11b supplement. Wireless LAN Medium Access Control (MAC) and Physical Layer (PHY) specifications. Higher-speed physical layer in the 2.4 GHz band, August 1999.

[24] IEEE standard 802.11a supplement. Wireless LAN Medium Access Control (MAC) and Physical layer (PHY) specifications. High-speed physical layer in the 5 GHz band, July 1999.

[25] IEEE standard 802.11g supplement. Wireless LAN Medium Access Control (MAC) and Physical layer (PHY) specifications. Further higher data rate extension in the 2.4 GHz band, April 2003.

[26] H. Jafarkhani. *Space-time coding: theory and practice*. Cambridge University Press, 2005.

[27] C.E. Shannon. A mathematical theory of communication. *ACM SIGMOBILE Mobile Computing and Communications Review*, 5(1):3–55, 2001.

[28] G.J. Foschini and M.J. Gans. On limits of wireless communications in a fading environment when using multiple antennas. *Wireless Personal Communications*, 6(3):311–335, 1998.

[29] R.W. Heath and A.J. Paulraj. Switching between diversity and multiplexing in MIMO systems. *IEEE Transactions on Communications*, 53(6):962–968, 2005.

[30] V. Tarokh, N. Seshadri, and A.R. Calderbank. Space-time codes for high data rate wireless communication: performance criterion and code construction. *IEEE Transactions on Information Theory*, 44(2):744–765, 1998.

[31] E. Biglieri, A. Constantinides, A. Goldsmith, A. Paulraj, and R. Calderbank. *MIMO wireless communications*. Cambridge University Press, 2007.

[32] W. Yu and JM Cioffi. Trellis precoding for the broadcast channel. *IEEE GLOBECOM'01 Global Telecommunications Conference*, 2, 2001.

[33] T.A. Wysocki and H.J. Zepernick. Characterization of the indoor radio propagation channel at 2.4 GHz. *Journal of Telecommunications and Information Technology*, 1(3-4):84–90, 2000.

[34] D. Gesbert, M. Shafi, D. Shiu, P.J. Smith, and A. Naguib. From theory to practice: an overview of MIMO space-time coded wireless systems. *IEEE Journal on Selected Areas in Communications*, 21(3):281–302, 2003.

[35] A. Paulraj, R. Nabar, and D. Gore. *Introduction to space-time wireless communications*. Cambridge University Press, 2003.

[36] B. Hassibi and B.M. Hochwald. How much training is needed in multiple-antenna wireless links? *IEEE Transactions on Information Theory*, 49(4):951–963, 2003.

[37] V.K. Jones, Greg Raleigh and Richard van Nee. MIMO answers high-rate WLAN call. Available in `http://www.eetimes.com/showArticle.jhtml?articleID=17200165`.

[38] L.U. Choi and R.D. Murch. A transmit preprocessing technique for multiuser MIMO systems using a decomposition approach. *IEEE Transactions on Wireless Communications*, 3(1):20–24, 2004.

[39] T.M. Cover and J.A. Thomas. Elements of Information Theory, 1991. *New York*.

[40] I.E. Telatar. Capacity of multi-antenna Gaussian channels. *European Transactions on Telecommunications*, 10(6):585–595, 1999.

[41] J.G. Proakis et al. *Digital communications*. McGraw-Hill New York, 1989.

[42] M. Aziz, M. Butler, A. Doufexi, A. Nix, and P. Fletcher. Indoor throughput and range improvements using standard compliantAP antenna diversity in IEEE 802.11 a and ETSI HIPERLAN/2. *IEEE VTS 54th Vehicular Technology Conference (VTC'01)*, 4, 2001.

[43] J.D. Moreira, V. Almenar, J.L. Corral, S. Flores, A. Girona, and P. Corral. Diversity techniques for OFDM based WLAN systems. *The 13th IEEE International Symposium on Personal, Indoor and Mobile Radio Communications*, 3:1008–1011, september 2001.

[44] X. Ouyang, M. Ghosh, and J.P. Meehan. Optimal antenna diversity combining for IEEE 802.11 a system. *IEEE Transactions on Consumer Electronics*, 48(3):738–742, 2002.

[45] N. Jindal. MIMO Broadcast Channels with Finite Rate Feedback. *IEEE Transactions on Information Theory*, 53(8):5045 – 5060, November 2006.

[46] M.H.M. Costa. Writing on dirty paper. *IEEE Transactions on Information Theory*, 29(3):439–441, 1983.

[47] http://www.itu.int/net/home/index.aspx.

[48] Andre Heck. *Introduction to Maple (3rd ed.)*. Springer-Verlag, New York, 2003.

[49] IEEE standard 802.11e supplement. Wireless LAN Medium Access Control (MAC) and Physical layer (PHY) specifications MAC enhancements for QoS, 2005.